Research Square

Preprints are preliminary reports that have not undergone peer review.
They should not be considered conclusive, used to inform clinical practice,
or referenced by the media as validated information.

Metaheuristic-Optimized Machine Learning Models for Predicting Shear Strength of Circular Concrete-Filled Steel Tubes with SHAP-Based and PDP Interpretability

Sourov Paul
Leading University
Pobithra Das
Leading University
Md Khaled Ahmed
Ahsanullah University of Science and Technology
Asmaul Husna Chara
Karadeniz Technical University (KTÜ)
Abul Kashem
Leading University
Mahmudul Haque Jamil
Leading University
Hafiz Farooq Ahmed
CCSIT, King Faisal University
Md Ehtesamul Haque
CCSIT, King Faisal University
Rama Samy Naidu
CCSIT, King Faisal University
Ammar Fayez Alshayeb
King Faisal University
Ziad Shatnawi
King Faisal University
Muhammad Imran Khan
Imam Mohammad Ibn Saud Islamic University (IMSIU)
Abdulrahman Fahad Alfuhaid
King Faisal University
Md Arifuzzaman
marifuzzaman@kfu.edu.sa

King Faisal University

Article

Keywords: Circular Concrete-filled Steel Tubes (CFSTs), Shear Strength, Particle Swarm Optimization, Bayesian Optimization, SHapley Additive exPlanations, Partial Dependence Plot, and Graphical User Interface

Posted Date: August 3rd, 2026

DOI: https://doi.org/10.21203/rs.3.rs-10211251/v1

License: This work is licensed under a Creative Commons Attribution 4.0 International License. Read Full License

Additional Declarations: No competing interests reported.

Metaheuristic-Optimized Machine Learning Models for Predicting Shear Strength of Circular Concrete-Filled Steel Tubes with SHAP-Based and PDP Interpretability

Sourov Paul[a], Pobithra Das[a], Md Khaled Ahmed[b], Asmaul Husna Chara[c], Abul Kashem[a], Mahmudul Haque Jamil[a], Hafiz Farooq Ahmed[d], Md Ehtesamul Haque[e], Rama Samy Naidu[e], Ammar Fayez Alshayeb[f], Ziad Shatnawi[f], Muhammad Imran Khan[g], Abdulrahman Fahad Alfuhaid[f], Md Arifuzzaman[f*]

[a] Department of Civil Engineering, Leading University, Sylhet-3112, Bangladesh

[b] Department of Civil Engineering, Ahsanullah University of Science and Technology, Dhaka, Bangladesh.

[c] Department of Civil Engineering, Karadeniz Technical University (KTÜ), Trabzon, Türkiye

[d] Computer Science Department, CCSIT, King Faisal University, P.O. Box 400, Al-Ahsa, 31982, Saudi Arabia

[e] Department of Computer Science, CCSIT, King Faisal University, P.O. Box 380, 31982, Al-Ahsa, Kingdom of Saudi Arabia

[f] King Faisal University, Department of Civil and Environmental Engineering, College of Engineering, P.O. Box 380, Al-Ahsa 31982, Saudi Arabia

[g] Imam Mohammad Ibn Saud Islamic University (IMSIU), Riyadh, Saudi Arabia

*Corresponding Author: E-mail: marifuzzaman@kfu.edu.sa (Md Arifuzzaman)

Abstract

Shear strength is a critical parameter for CFSTs, as shear failure occurs abruptly and can compromise structural safety. Accurate prediction of the shear strength of circular concrete-filled steel tubes (CFSTs) is crucial for the safe and economical design of composite structural systems. Traditional empirical and analytical approaches often struggle to capture the nonlinear interactions between geometric, material, and loading parameters. This study introduces innovative metaheuristic-optimization-based machine learning models, particle swarm optimization (PSO) and Bayesian optimization (BO), enhanced by random forest (PSO-RF), category boosting (PSO-Cat), and random forest (BO-RF) and (BO-Cat), with a focus on the shear strength prediction of circular CFSTs. Hence, to assess the model performance, we used the R^2, RMSE, MAPE, and MAE metrics. A comprehensive experimental database was compiled from published literature and was divided into training (70%) and testing (30%) phases. The results demonstrate that the (PSO-Cat) and (BO-Cat) algorithms achieve excellent predictive accuracy among all the

evaluation metrics, with (R^2 = 0.999, RMSE = 19.6455) in the training stage and (R^2 = 0.9874, RMSE = 65.0769) in the testing stage (BO-Cat: R2 = 0.999, 0.9817), which exceeds those of the (PSO-RF) and (BO-RF) models. Additionally, SHapley additive exPlanations (SHAPs) and partial dependence plot (PDP) analyses were employed to identify significant input characteristics and the influence of input parameters on shear strength outcomes. The results demonstrate that the metaheuristic-optimized models significantly outperform conventional approaches in terms of prediction accuracy, whereas SHAP analysis highlights the dominant role of the concrete area (Ac), steel reinforcement area (As), and shear span-to-depth ratio (a/D) as the most impactful parameters in governing shear capacity. Furthermore, a graphical user interface (GUI) was developed to make the predictive models accessible for practical engineering use, allowing users to input design variables and obtain shear–strength predictions with interpretability features. This research provides a reliable, interpretable, and deployable framework for predicting the shear strength of CFSTs.

Keywords: Circular Concrete-filled Steel Tubes (CFSTs), Shear Strength, Particle Swarm Optimization, Bayesian Optimization, SHapley Additive exPlanations, Partial Dependence Plot, and Graphical User Interface

Abbreviations: CFSTs, Circular Concrete-filled Steel Tubes; SFRC, Steel fiber-reinforced Concrete; ST, Shear Strength; SFRC, Steel fiber-reinforced Concrete; FRRRAC, Fiber-reinforced Rubberized Recycled Aggregate Concrete; AASHTO, American Association of State Highways and Transportation Officials; BDS, Bridge Design System; WSDOT, Washington State Department of Transportation; PSO, Particle Swarm Optimization; BO, Bayesian Optimization; RF, Random Forest; CatBoost, Category boosting; LR, linear regression; GEP, Gene Expression Programming; SVR, Support Vector Regression; GBR, Gradient Boosting Regression; ANN, Artificial Neural Networks; SHAP, SHapley Additive exPlanations; PDP, Partial Dependence Plot; GUI, Graphical User Interface;

1. Introduction

Concrete-filled steel tubes (CFSTs) have become popular as a preferred alternative in modern construction because of their better durability and flexibility[1]. A CFST is composed of a hollow steel tube that is packed with concrete, allowing the composite structure to leverage the optimal characteristics of both materials. The steel framework exerts confining pressure on the core concrete, which improves its compressive strength, whereas the concrete core mitigates local buckling of the steel tube [2]. Hence, this synergy results in high load-bearing capacity, improved ductility, and excellent energy dissipation, making CFSTs particularly suitable for high-rise buildings, bridges, and seismic-resistant structures [3]. Among various shapes, circular CFSTs are

frequently favored because of the uniform confinement provided by the steel tube to the core concrete. Compared with square or rectangular sections, this design results in increased axial and shear resistance [4]

One critical parameter in the design and safety assessment of CFST members is their shear strength. Although the axial and flexural capacities of CFSTs have been extensively studied, very few studies have been conducted on shear strength prediction [5]. However, in seismic-prone regions or structural elements subjected to combined loading, shear plays a vital role in preventing brittle failure [6]. Shear strength refers to a material's capacity to tolerate shear stress until it experiences plastic failure in shear. The calculation is derived from the largest force observed during a torsional test and is reliant upon the initial cross-sectional area of the sample being tested [7]. Multiple competing methods exist for measuring shear strength (τ), involving case-by-case selection, as not all shear testing methods result in shear failure. The shear strength is calculated by dividing the force at separation by the entire zone of the section being sheared [8]. Concrete exhibits shear weakness due to its insufficient tensile strength. The goal of designing a strengthening shear system is to counteract the applied force of shear that remains [9].

A steel–concrete composite component reduces the internal buckling of a tube [10,11]. Ye et al. [12] investigated the impact of material and geometric properties. The study revealed that both square and circular members exhibited observable ductile behavior. Using two different kinds of concrete fill, Xu et al. [13] conducted seventy tests on circular members. Expansive concrete fill significantly increased the shear capacity. Furthermore, these equations are often derived under restrictive assumptions and limited experimental datasets, making them inadequate for capturing the complex interactions among geometric parameters, material properties, and loading conditions [14]

Research on high-strength rectangular CFST shorter columns [15], highly durable circular shortened columns [16], and robust rectangular beams [17] has been conducted in earlier studies. Lehman et al. [18] studied 22 large-scale samples to investigate the impacts of the shear span ratio, tube diameter to thickness ratio, tail length, concrete compressive strength, and interface conditions. Alghossoon et al. [19] noted that most numerical software is unable to accurately represent the behavior of concrete in orthogonal directions because of its complex shear behavior. A database of rectangular CFST columns with high strength was developed by Lai and Varma (2015) [4]. Additionally, they developed a resistance factor and new design equations for calculating cross-sectional strength through finite-element parametric analysis. However, it takes considerable time and money to construct trustworthy FE models. The type of column capacity prediction mentioned above requires robust data-driven models. AASHTO BDS [20], Eurocode [21], WSDOT [22], and CECS [23] were among the design provisions that were assessed in relation to the estimation of shear strength in HS-CFST members. There is no formula for calculating the shear strength of a composite type in the AASHTO BDS [20]. Simple bending

configurations with basic end supports under repeated loading were used in the majority of studies on the shear strength of composite CFSTs and RCFSTs [13,24,25].

Deep learning networks trained on labeled images for predicting the shear behavior of concrete-filled steel tubular members have been extensively researched in recent years. Although shear behavior forecasting has improved significantly through the development of machine learning and artificial neural network models, integrating these models into various CFST configurations and material properties remains challenging. Machine learning approaches, including random forest (RF), XGBoost, support vector regression (SVR), gradient boosting regression (GBR), and artificial neural networks (ANNs), have been used to estimate the shear strength of this structural member type accurately. With R^2 values of 0.776 or 0.768 for elliptical CFST columns, the hybrid approach performed better than did previous methods [26]. According to previous studies, combined methods such as GBR and XGBoost typically yield the best predictive accuracy, with R2 values exceeding 0.98 [27]. These results not only improve the accuracy of shear capacity predictions but also provide practical guidance for enhancing CFST design in engineering applications [28]. However, owing to the interactions between materials (steel and concrete) and structural features, it is difficult to predict the shear behavior of a CFST. Existing empirical models typically fail to incorporate these details, leading to prediction mistakes [29].

1.2 Literature review

Machine learning approaches have recently emerged as promising options for forecasting the mechanical properties of concrete materials and structural elements. These forecasting techniques can reduce time, labor, and money by providing the desired characteristics of experimental or numerical research. The mechanical properties of concrete can be properly predicted via machine learning, which has been a significant issue for both research and practical applications [30]. FR3C (fiber-reinforced rubber recycled aggregate concrete) is made of materials that are recognizable to the concrete industry, considering that both rubber waste and fiber components have specific mechanical properties. For concrete to achieve the required compressive strength, the mix design is crucial and depends on the interactions between components, which many machine learning models can predict with ease. According to the findings of Avijit et al. [31], who utilized 905 experimental data points, the CatBoost model appears to be the most accurate for forecasting the compressive strength of FR3C, with the greatest R^2 of 0.865. According to Piyu et al. [32], on the basis of machine learning research findings, the gene expression programming or GEP model outperforms linear regression (LR) and nonlinear regression (NLR) equations, exhibiting a set of overfitting issues concerning accuracy, generalization, and predictive capability. The GEP model's objective function was found to be 25% and 33% more effective than those of the LR and NLR models, respectively. Amedeo et al. [33] also reported that the Gaussian process regression (GPR) model outperformed the support vector machine (SVM) model in predicting the compressive strength of rubberized concrete. Artificial neural network (ANN) models can be built with different

architectural approaches, including hidden neurons or layers, and can be altered for research to enable multiple physical property predictions.

To identify the design relationship between several environmentally friendly rubberized concrete mix combinations and their multiple physical characteristics simultaneously, the ML model of an artificial neural network (ANN) can be established. An MSE value of 7.2420 and an R^2 value of 0.9710 were used to evaluate the efficiency of the optimal ANN architecture as satisfactory, as reported by Xu et al. [34]. Miljan et al. [35] reported that the compressive strength of self-compacting rubberized concrete (SCRC) can be estimated via machine learning techniques, and MLP-ANN ensembles achieved the best prediction accuracy, with a mean absolute error (MAE) of 2.81. Compared with regular concrete, the incorporation of discontinuous fibers improves the performance of steel fiber-reinforced concrete (SFRC). For estimating the compressive and flexural strengths of SFRC, the best machine-learning techniques are XGBoost and gradient boosting regression [36]. Using a total of 443 experimental datasets, Samia et al. [37] reported that random forest was the most effective machine learning model, achieving the highest R^2 value of 0.88. According to machine learning models, the number of bolt rows and the steel ultimate-to-yield strength ratio, which are currently disregarded by design regulations, have considerable impacts on the bearing strength of double-shear bolted connections. To identify the failure modes of double-shear bolted joints, Samia et al. [38] also evaluated 10 machine learning techniques on a large database of 455 experimental findings. The random forest model outperformed the other models, achieving accuracies of 92% and 99% for the testing and training datasets, respectively. A user interface that gathers suggested machine learning models can be subsequently developed. Advanced concrete composites have been increasingly used as effective techniques for strengthening reinforced concrete structural components, such as beams.

Machine learning techniques are rather accurate in forecasting the shear strength of RC beams reinforced with inorganic composites. According to Tadesse et al. [32], the XGBoost model provides the most accurate predictions, with an R2 value of 0.995, which is the highest. To distribute force while maintaining the frame's stability during earthquakes, beam–column joints are crucial. Failures of beam–column joints can cause structures to collapse completely or partially. The potential beam–column joint failure modes were predicted by Xiangling et al. [33] via machine learning on 580 test data, and the XGBoost approach should be considered in this case because of its improved classification performance for beam–column joint failure modes, which achieves 91% accuracy. One of the most common failures to consider in the design of concrete beams is shear failure. The shear capacity of steel fiber-reinforced concrete beams without web reinforcement can be reliably predicted via machine learning techniques. In the study by Jesika et al. [34], 507 experimental data points were used for the ML approach, and the XGBoost model proved to be the most effective, with a mean absolute error of 0.704, the lowest. Estimating the structural behavior of buildings under seismic ground motions is one of the most significant yet difficult scientific problems in earthquake engineering. It is possible to anticipate seismic impacts

on RC buildings via a fully verified, interpretable machine learning algorithm [39]. The mode of failure of shear walls can also be predicted via open-source, data-driven machine learning classification algorithms. Sujith et al.'s [40] study compiles a comprehensive database of 393 test outcomes across 8 machine learning models. The results revealed that the random forest model had the best accuracy of 86%. There is no specific method for predicting the seismic responses of RC buildings because earthquakes impose highly variable external loads because of their complexity and unpredictability. By analyzing 165 RC frame structures, Kazemi et al. [37] demonstrated that existing or newly built RC buildings may incorporate their seismic limit-state capacity, and their performance can be evaluated via artificial neural networks and an XGBoost model.

A large database of 719 tests from [41] revealed that the LightGBM and CatBoost models outperformed the other methods in terms of their ability to predict the capacity of CFST columns, with accuracies of 97.9% and 98.3%, respectively. The work of Javed et al. 2020 [42] uses 227 data samples to derive the expression for determining the maximum axial strength of CFST long round columns via gene expression programming, also known as GEP, which is a new, well-known technique[43]. Le et al. 2022 [44] utilized a dataset of 880 experimental tests to construct a new and useful equation based on an artificial neural network (ANN) for estimating the axial load of rectangular concrete-filled steel tubular columns. According to Ahmadi et al. 2017 and Bardhan et al. 2022 [45,46], the ML model of an artificial neural network (ANN) is accurate and effective at predicting the properties of circular concrete-filled steel tube (CCFT) columns. With a total of 220 data samples, the results of Deng et al. 2024 [47] demonstrate that the random forest model's predictions achieve the best overall performance in forecasting the final concrete-filled steel tube stub column bearing capacity. The Gaussian processing regression (GPR) model had the maximum effectiveness in predicting the shear capacity of circular concrete-filled tubes (CCFTs), with an average error of 0.5% in the study of [48], which employed 141 experimental test results. Using the results of 230 tests, Mansouri et al. 2024 [49] reported that the XGBoost model was the most accurate ML model for estimating the shear strength of concrete-filled steel tubes, with an R^2 value of 0.986. In addition to the largest shear test database for both circular and square CFST columns, which includes 314 good-quality datasets, the work of [50] employs a Bayesian model updating technique. With Bayesian posterior models producing R^2 values of 0.970 and 0.975, the suggested Bayesian model update strategy performs exceptionally well.

1.3 Significance of this Research

The shear strength prediction of circular concrete-filled steel tubes (CFSTs) is critical for ensuring the safety, reliability, and cost effectiveness of composite structural systems. Since shear failure occurs suddenly and can lead to catastrophic structural consequences, accurate estimation of this parameter is essential for both design and performance evaluation. However, traditional empirical formulations and analytical models often fail to capture the highly nonlinear interactions among

material properties, geometric parameters, and loading conditions. This limitation not only restricts the prediction accuracy but also hinders the practical application of such models in modern structural design.

The present study addresses this gap by integrating metaheuristic-optimization-based machine learning models with advanced interpretability techniques. Compared with conventional methods, the development of hybrid frameworks such as PSO-Cat, PSO-RF, BO-Cat, and BO-RF significantly enhances prediction accuracy, as demonstrated by superior performance metrics. In addition to predictive accuracy, incorporating SHAP and PDP analysis provides crucial interpretability, enabling engineers to identify the most influential parameters, such as the concrete area, reinforcement area, and shear span-to-depth ratio, that govern shear strength. This enhances confidence in model outputs and facilitates knowledge-driven engineering decisions. Additionally, the creation of a graphical user interface (GUI) makes these models practically deployable, bridging the gap between advanced computational intelligence and day-to-day structural engineering practice. In the final analysis, this research contributes not only to the development of computer modeling but also to the creation of tools that reduce costs, improve safety, and encourage the adoption of intelligent design approaches in structural engineering.

2.0 Data description

In the present study, datasets collected from previously published research were used to generate predictions with popular hybrid machine learning (ML) models. Published studies have provided the strength parameters of the mixtures used in circular concrete-filled steel tube (CFST) samples. A database was created from 230 shear–strength experiments published in the literature[51–55]. The data collection was divided into two phases: training and testing. Seventy percent of the dataset was allocated for model training, whereas the remaining 30% was reserved for testing. In the initial stages, the AI models were trained to predict outcomes with a certain level of accuracy. The goal of the testing phase was to assess whether the algorithms could accurately forecast results when presented with diverse data inputs [56,57]. **Table 1** presents the general parameters of the samples, such as their geometrical features, material properties, applied axial loads (P), and shear strength measurements (Vtest), which were collected from various sources and organized in a database. Among the geometric properties were the specimen's cross-sectional diameter (D), the tube's thickness (t), and the shear span length to cross-sectional diameter ratio (a/D). The material properties included the yield stress (Fy) and compressive strength (fc) of the steel. The author of this study chose the following input parameters for advanced machine learning approaches: the cross-sectional area of the concrete core (Ac), the cross-sectional area of the steel tube (As), the yield stress of the steel (Fy), the ratio of the shear span length to the cross-sectional diameter (a/D), the ratio of the applied axial load to the axial compressive strength (P/P0), and the cylindrical compressive strength of the concrete (fc). Additionally, according to AISC 360-22, P0 was collected in this study. Specifically, it was estimated that, in these situations, the cylindrical compressive strength (fc) was approximately 0.8 times the cubic compressive strength.

Figure 1 shows a heatmap of the Pearson correlation coefficients between predictor variables and the target output, Vtest (shear strength measurement), for circular concrete-filled steel tubes (CFSTs). The strongest positive correlations with the model's shear strength predictions are with the steel tube's cross-sectional area Ast (r=0.90) and the concrete core Ac (r=0.81). This highlights the dominant influence of the structure's geometric size on its shear capacity. Additionally, the shear strength is moderately positively correlated with the cylindrical compressive strength of the concrete, fc (r=0.32). Conversely, the yield stress of steel, Fy (r= -0.22), and the ratio of the shear span length to the cross-sectional diameter, a/D (r= -0.13), have weak negative correlations with the shear strength. Furthermore, Ast and Ac exhibit a high level of multicollinearity (r=0.80), indicating that these two key input characteristics should be considered together when developing an effective machine learning model.

Table 1: Statistical summary of the input and output variables.

	Ast mm^2	Ac mm^2	a/D	P/P0	Fc MPa	Fy MPa	Vtest KN
Data Point	230.0	230.0	230.0	230.0	230.0	230.0	230.0
Mean	2433.86	29263.513	0.259	0.255	39.313	373.091	870.842
std	1486.741	29263.51	0.136	0.223	12.116	66.634	602.416
Min	741.04	9116.56	0.075	0	19.2	276.8	240
25%	1526.04	17436.11	0.14	0	29.5	330	435.625
50%	2191.79	19855.07	0.25	0.253	35.99	346.95	627.5
75%	3184.91	25164.2	0.386	0.453	46	408	1210.5
Max	10002.4	192669.8	0.5	0.85	67.5	549	3569
Median	2191.79	19855.07	0.25	0.253	35.99	346.95	627.5
Mode	3184.91	67497.32	0.3	0	25.9	307.6	495
Kurtosis	10.532	15.638	-1.058	-0.753	-0.123	1.208	4.214
Skewness	2.645	3.529	0.496	0.411	0.847	1.325	1.775

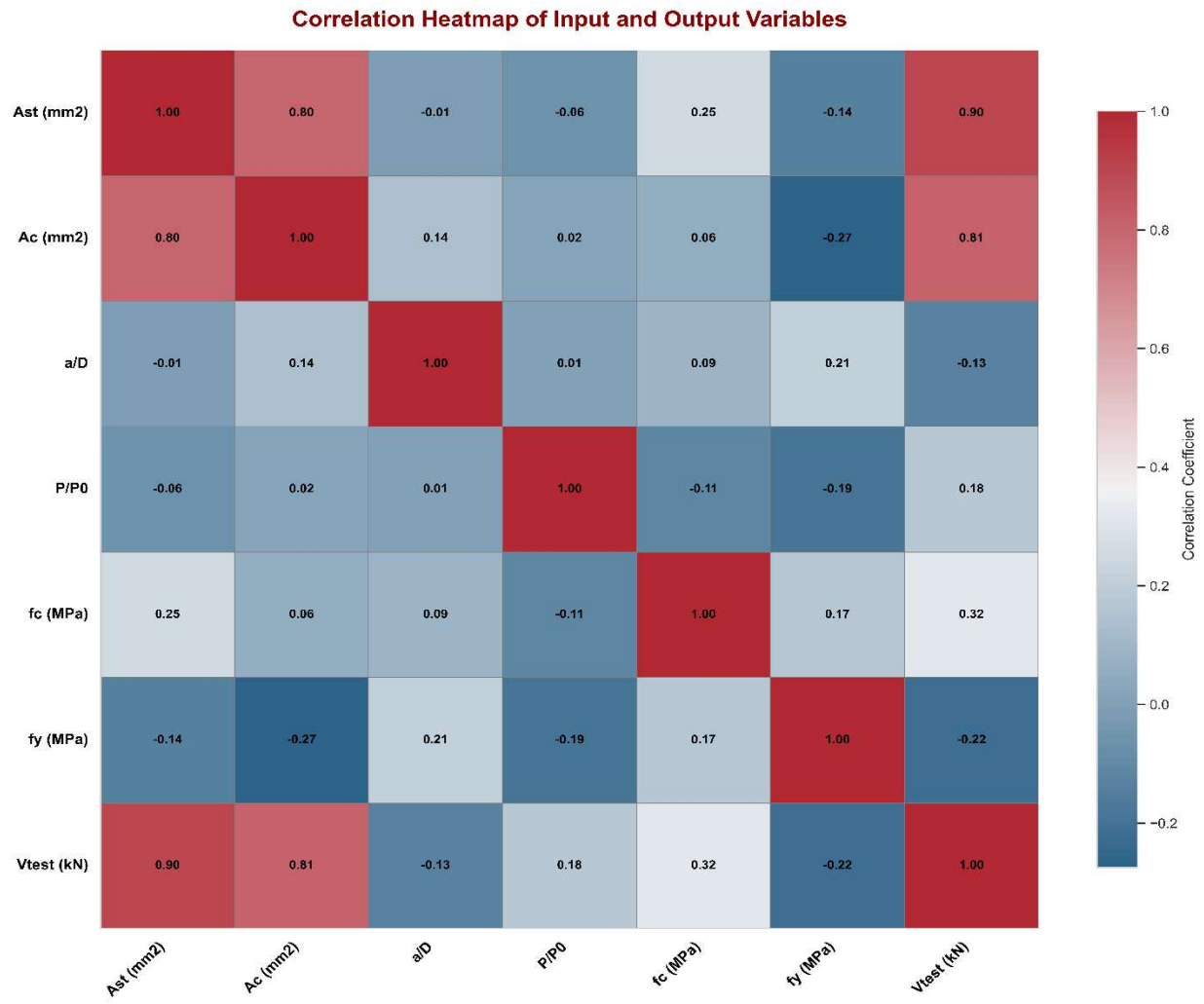


Figure 1. Heatmap showing the linear one–to–one correlation between variables.

3. Methodology

3.1 CatBoost Model

CatBoost is an advanced machine learning tool that falls within the gradient boosted decision tree (GBDT) group and is especially effective at handling categorical features; it was developed by Yandex in 2018 [58]. This model was originally developed to address issues such as overfitting, prediction shift, and gradient bias commonly encountered in traditional boosting techniques [59]. CatBoost was developed for both classification and regression tasks, including complex applications such as evapotranspiration estimation, aboveground biomass prediction, and corporate failure modeling [60]. It is particularly suitable for noisy, heterogeneous datasets [61]. The model processes data by transforming categorical variables into numerical values via target

statistics and performing ordered boosting to reduce overfitting [60]. It constructs symmetric decision trees (oblivious trees) and integrates category-based information directly into its learning process, requiring minimal preprocessing [62]. CatBoost has achieved high accuracy across multiple domains. For example, it achieved a lower RMSE than random forest and XGBoost in forest biomass prediction and surpassed 97% accuracy in corporate risk forecasting [60]. The key equation used in processing categorical features is as follows:

$$x_k^i = \frac{\sum_{j=1}^{P-1}[X_{jk}=X_{jk}]*Y_j+\alpha*p}{\sum_{j=1}^{P-1}[X_{jk}=X_{jk}]+\alpha} \quad \text{Equation 1}$$

where x_k^i= the new numeric value for the categorical feature k of data point i and where X_{jk}= the value of the K^{th} feature for the j^{th} data point (in training data). Similarly, X_{jk} represents the value of the k^{th} feature for the current (i-th) data point. $[X_{jk} = X_{jk}]$ = an indicator function (1 if values match, 0 otherwise), and Y_j denotes the label (target value) of the j^{th} training data point. *P,* the prior, is usually the average label across the entire dataset. α =The smoothing parameter (also called the regularization weight) balances the influences of the prior and actual data. *P:* The total number of permutations or orderings used for this feature during training. CatBoost consistently achieves higher accuracy and lower error rates than traditional models such as random forest, SVM, and XGBoost [62].

3.2 Random forest regression (RFR)

Leo Breiman unveiled random forest regression (RFR) in 2001, an ensemble machine learning model that uses many decision trees [63]. It is designed for both classification and regression tasks, with strong performance in high-dimensional and nonlinear data settings[64]. In regression, RFR builds many trees via different subsets of data and predictor variables, a process known as bootstrapping and feature randomness [65]. These trees work independently, and their predictions are averaged to produce the final output, reducing overfitting and improving stability [66]. RFR has been applied in fault detection in power systems and landslide susceptibility mapping [67]. The model effectively handles missing or noisy data and performs well in real-world scenarios. Its prediction process relies on ensemble learning approaches and typically involves averaging. One key formulation is as follows:

$$Y = \frac{1}{T}\sum_{t=1}^{T} P(\frac{y}{x, P_t}) \quad \text{Equation 2}$$

where T is the total number of trees, and $P(\frac{y}{x,P_t})$ is the assessment of the results from tree t. OOB error estimation and the RMSE are commonly used to evaluate model accuracy [68].

3.3 Particle swarm optimization (PSO)

In 1995, Kennedy and Eberhart developed Particle Swarm Optimization (PSO), an optimization approach inspired by nature. It drew its inspiration from bird groups or fish schools for sustenance [69]. The concept of PSO originated from early research on social interaction. It was originally designed for animation work, but it soon became a useful tool for tackling tough optimization issues [70]. Engineering, medicine, and control systems are just a few of the many areas where this approach is widely applied. In particular, when the search space is vast and conventional techniques have trouble locating acceptable solutions, it is useful [71].

PSO acts by modeling a swarm or a cluster of particles. Each particle stands for a potential solution and has a velocity and a position [72]. The best solution for the swarm overall (global best) and the best account is made of the solution each particle has found (personal best). They slowly change into higher positions [73]. The movement of each particle is updated via the following formula:

$$\vartheta t + 1 = \omega\vartheta t + c_1 r_1 (P - x) + c_2 r_2 (G - x), x_{t+1} = x_t + \vartheta_{t+1} \quad \text{Equation 3}$$

where r1 and r2 are random variables, C1 and C2 are learning rate functions, and ω is the total inertia weight. This equation includes weights and random factors that help balance exploration and precision. PSO often yields very accurate results, although it can sometimes settle too early on suboptimal answers. Researchers have improved it by using small tweaks such as inertia or hybrid models to make it more reliable [74].

3.4 Bayesian optimization

Bayesian optimization, or BO, is a sophisticated method for tackling optimization problems where the function to be optimized is unknown and costly to evaluate. Consider situations where every test or experiment takes time or money. BO helps by building an intelligent guess, or model, about how the function behaves. This model does not just guess the value at a new point; it also tells you how uncertain it is about that guess, which is useful for deciding where to try next [75]. BO often uses a technique called a Gaussian process (GP) to make these predictions. Additionally, any new input parameter x_{t+1} estimates the expected value $\sigma^2(x_{t+1})$ as follows:

$$\mu(x_{t+1}) = k^T k^{-1} f_{1:t}, \sigma^2(x_{t+1} = k(x_{t+1,} x_{t+1}) - k^T K^{-1} k \quad \text{Equation 4}$$

In plain terms, these calculations help BO decide whether it should explore unknown regions or focus on promising spots. BO's roots go back to early work by Kushner, and it received a boost with the efficient global optimization framework [76]. It has been used in many areas—from finding new materials to designing neural networks—because it balances searching for better options while learning from past tests. The method uses a combined function to select another sample point, balancing the exploration of uncertainty and the exploitation of good areas. A related process, the Bayesian optimization algorithm (BOA), takes a slightly different approach by

modeling relationships between variables with Bayesian networks [77]. The probability function solution X = ($X_{1,\ldots,}X_n$) is calculated as follows:

$$P(X) = \prod_{i=1}^{n} P(X_i | \prod\nolimits_i) \quad \text{Equation 5}$$

where $\prod_i$, represents the parent variables, including X_i. The BOA evaluates these models via Bayesian scoring methods. The idea behind BO dates back to Thompson's work in 1933 and was later refined through experimental design principles [78]. Its main goal is to find the input.

$$x^* = \arg\max f(x)/x\epsilon X \quad \text{Equation 6}$$

After each evaluation, the model updates, and the acquisition function, such as expected improvement (EI), determines where to focus next.

$$\alpha_{EI}(x) = (\mu_n(x) - \tau)\phi\,(\tfrac{\mu_n(x)-\tau}{\sigma_n(x)}) + \sigma_n(x)\emptyset\,(\tfrac{\mu_n(x)-\tau}{\sigma_n(x)}) \quad \text{Equation 7}$$

τ is the best value found thus far, and ϕ and θ are standard normal distribution functions. In this way, BO smartly focuses on regions likely to improve the results [78]. Finally, BO is especially useful for tuning machine learning models when gradients are not available and evaluations are expensive. It usually finds good solutions faster and with fewer tests than traditional methods do, which makes it very practical [79].

3.5 SHapley Additive exPlanations (SHAP)

An approach for comprehension based on cooperative game theory is known as SHapley Additive exPlanations (SHAP), which assigns a fair contribution to each feature in a machine learning model. This approach facilitates local explanations for specific predictions as well as global explanations encompassing all data points. This makes it suitable for analyzing complex "black box" algorithms [80]. The SHAP framework calculates a linear function of inputs:

$$g(x') = \emptyset_0 + \sum_{i=1}^{M} \emptyset_i\, x_i' \quad \text{Equation 8}$$

where x' represents the simplified function input, *M* represents the input features, $\emptyset_0$ represents the baseline prediction, and $\emptyset_i$ represents the Shapley value of feature *i* [81]. To achieve distinct and trustworthy feature attributions, the Shapley values guarantee local precision, robustness to missing values, and consistency. The function of the Shapley value feature i is mathematically expressed as:

$$\emptyset_i = \sum_{S \subseteq N\{i\}} \frac{|S|!\,(|N| - |S| - 1)!}{|N|!} [\vartheta(S \cup \{i\}) - \vartheta(S)] \quad \text{Equation 9}$$

where N is the set of functions and where $\vartheta(S)$ is the model prediction with subset S [82]. This method emphasizes biases or anomalies in the model's behavior, improves interpretability, and enables the identification of important predictors [83]. SHAP can also be utilized with neural networks and tree-based models in engineering applications [84].

3.6 Partial dependence plot (PDP)

Partial dependence plot (PDP) analysis is a crucial resource for understanding machine learning. It shows how a model's predictions change when one or two input features change by averaging the effects across the other features in the data points. [85,86]. Partial dependence plots, or PDPs, are mostly about determining a function that shows how much a feature affects a trained model's prediction on average, taking into account all the other features [87,88].

If the full feature set $x = (x_S, x_C)$, where x_S is the function or set of interest and x_C is the complement set of other features, is required for a trained prediction function f to function. The definition of the partial dependence function is as follows:

$$f_{x_s}(x_S) = E_{x_C}\left[f_{x_s}(x_S, x_C)\right] = \int f(x_S, x_C)\, dP(x_C) \qquad \text{Equation 10}$$

The x-axis of a PDP shows the values of the input feature that is being evaluated, and the y-axis shows the average effect of the outcomes, such as partial dependence. The y-axis provides the expected shear strength for the feature at different values.

3.7 Uncertainty Analysis

Uncertainty analysis is a valuable approach for assessing and quantifying the reliability of model predictions. This approach accounts for uncertainties in the input variables and examines how their functional propagation through the model ultimately affects the output. The present study used the uncertainty range to assess future variability in model predictions and to analyze potential model variations at the 95% confidence level. This method provides a detailed examination of the actual data and supports functional decision-making by accounting for the model's uncertainty.

$$U_{95} = 1.96\sqrt{SD^2 + RMSE^2} \qquad \text{Equation 11}$$

In this context, U95 quantifies the uncertainty associated with the ML approach, whereas RMSE denotes the root-mean-square error; similarly, SD indicates the standard deviation of the predictive error. U95 represents the 95% critical value of the standard normal distribution, with a lower U95 indicating a more reliable, higher-performing model.

3.8 Performance evaluation metrics

Modeling tools are increasingly effective at predicting shear strength in concrete-filled circular steel tubes. The appropriate evaluation parameters are significant for the calculation of these

models' outcomes. It assesses machine learning models' performance via various error and accuracy indicators. The four widely used metrics include the R-square (R^2), root mean square error (RMSE), mean absolute error (MAE), and mean absolute percentage error (MAPE) [89]. The coefficient of determination (R^2) indicates how well the model explains the reliability of the target function. A value approaching 1 indicates a better fit. The RMSE highlights the typical scale of prediction inaccuracies by squaring differences before averaging. The MAE provides an unambiguous measure of errors and is less affected by outliers. The MAPE is valuable for comparing models across different datasets or sizes, as it expresses error as a percentage, making it easier to compute the average absolute difference function between observed and expected values [90].

$$R^2 = 1 - \frac{\sum_{i=0(x_1 - x_2)}^{n} 2}{\sum_{i=0(x_1 - y)}^{n} 2} \quad \text{Equation 12}$$

$$\text{MAE} = \frac{1}{2} \sum |x_1 - x_2| \quad \text{Equation 13}$$

$$\text{RMSE} = \sqrt{\frac{1}{2}} \sum (x_1 - x_2)^2 \quad \text{Equation 14}$$

$$\text{MAPE} = \frac{1}{2} \sum \left| \frac{x_1 - x_2}{x_2} \right| \quad \text{Equation 15}$$

In the evaluation equations, x_1 represents the expected value, x_2 is the actual value, y denotes the mean of the actual values, and n is the total number of data points used in the analysis. In **Fig.2** display the research working process.

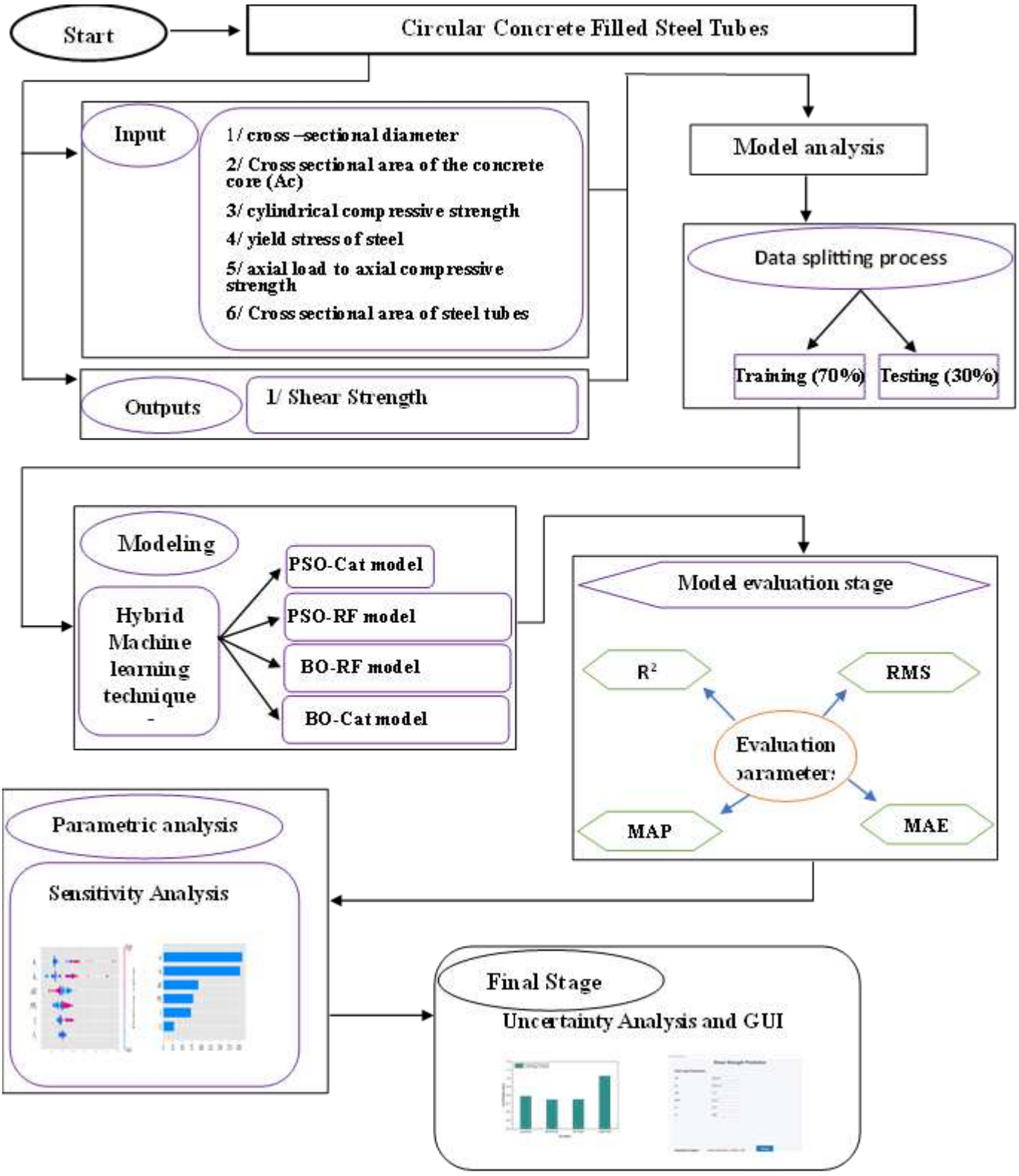


Fig. 2. Flowchart of this study

4. Results and Discussion

4.1. ML models' prediction performance

Figure 3 shows the distribution of prediction errors across the training and testing phases of four distinct (BO-Cat, BO-RF, PSO-Cat, and PSO-RF) machine learning models. The error values for each model are displayed via a combination of violin plots and box plots, emphasizing the density and distribution of mistakes. The data show that the maximum errors fall within an approximate range of +150--150 during the training stage, whereas during the testing phase, the errors are between approximately +180--180. Additionally, the BO-RF and PSO-RF exhibit wider error distributions and greater volatility during the training phase; the BO-Cat and PSO-Cat models exhibit a very narrow error range, from nearly +25--25, indicating better performance. Notably, the PSO-RF model maintains a symmetric error distribution during training despite a somewhat broader dispersion. All the models exhibit greater error variability during the testing phase, with BO-RF and PSO-RF again showing wider ranges. During testing, PSO-Cat and BO-Cat exhibit tighter clustering than the other two methods do, indicating greater generalizability reliability. Furthermore, in both phases, the BO-cat and PSO-Cat models provide the best overall balanced performance.

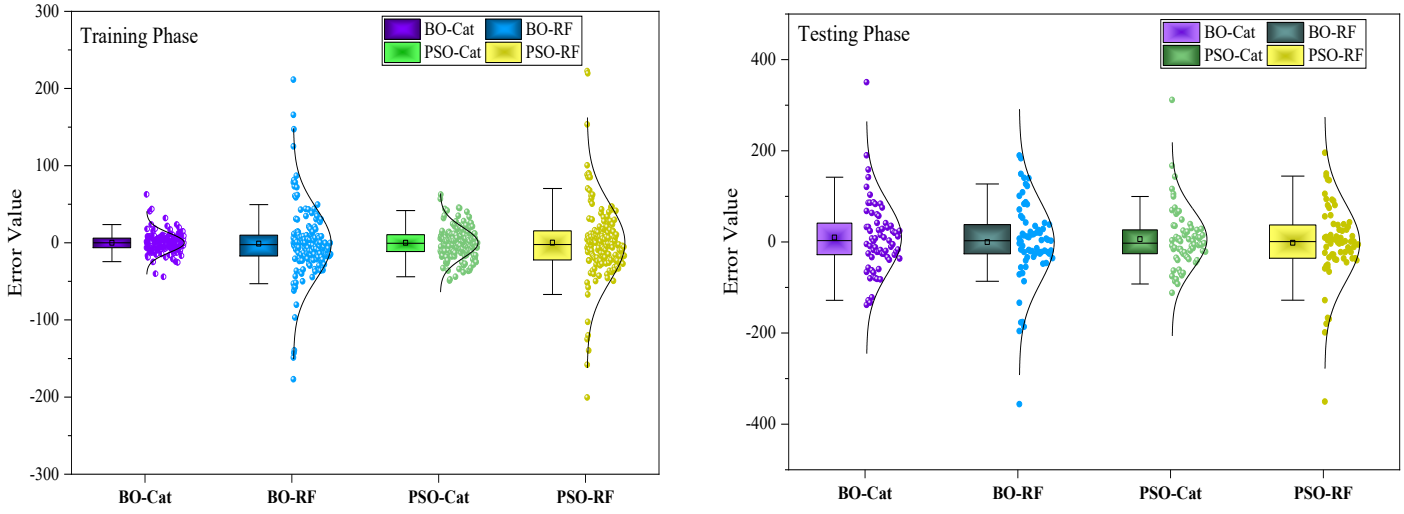


Figure 3. The error values of the ML techniques for shear strength prediction.

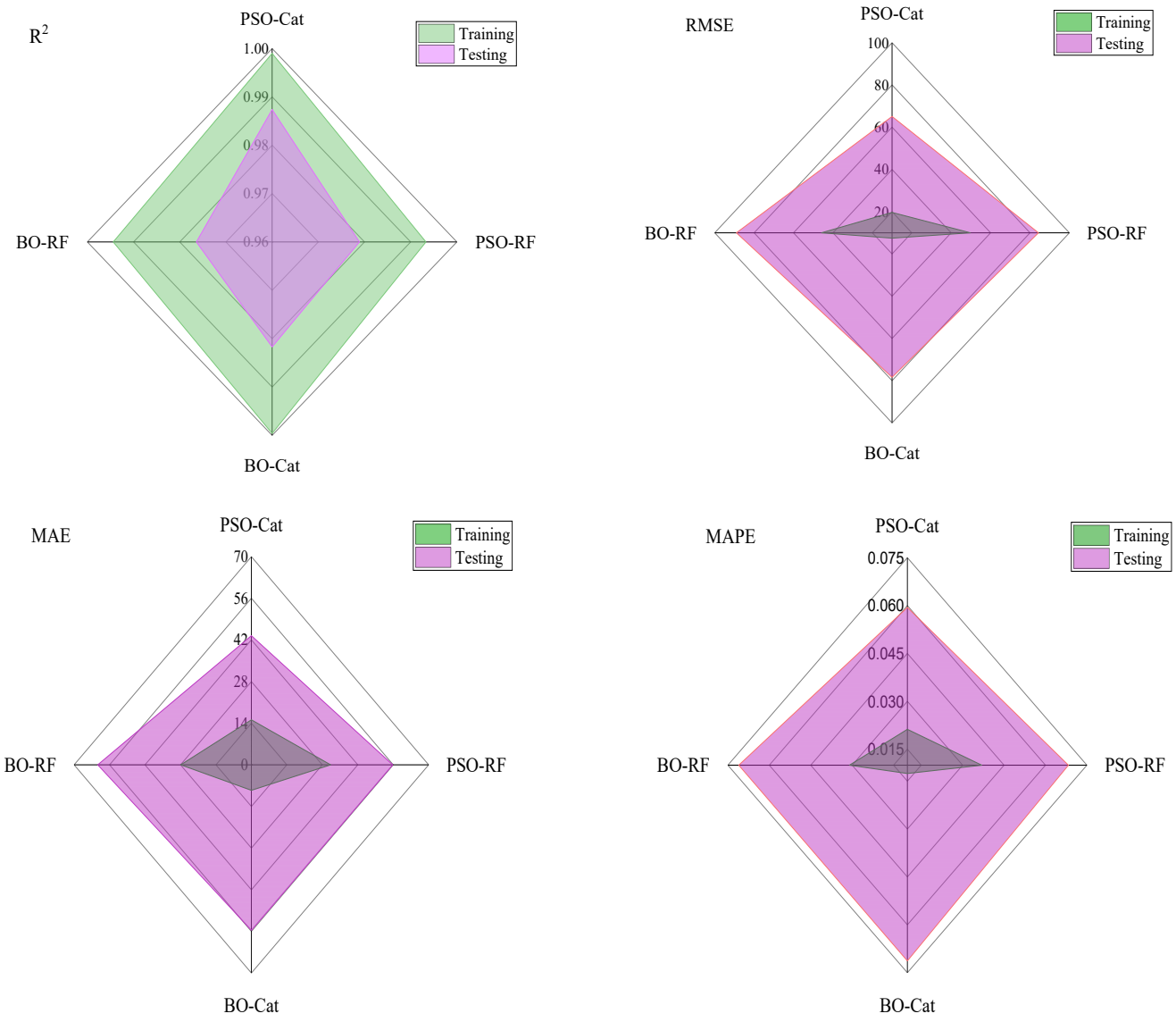


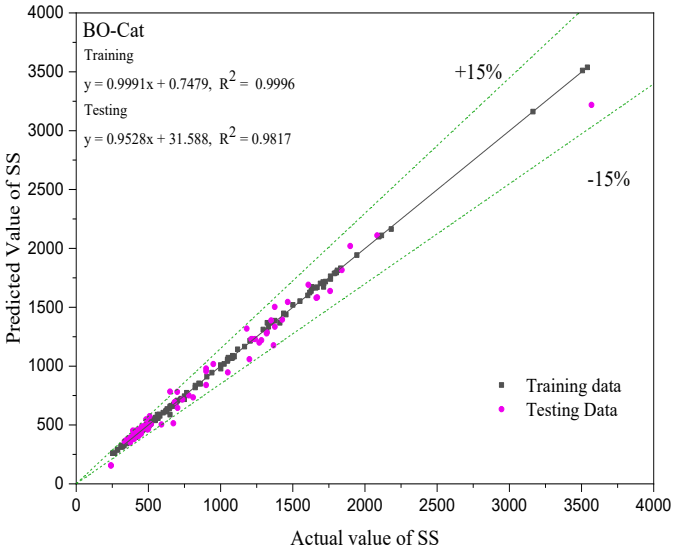
Figure 4. Radar plots of shear strength assessment of performance ML approaches.

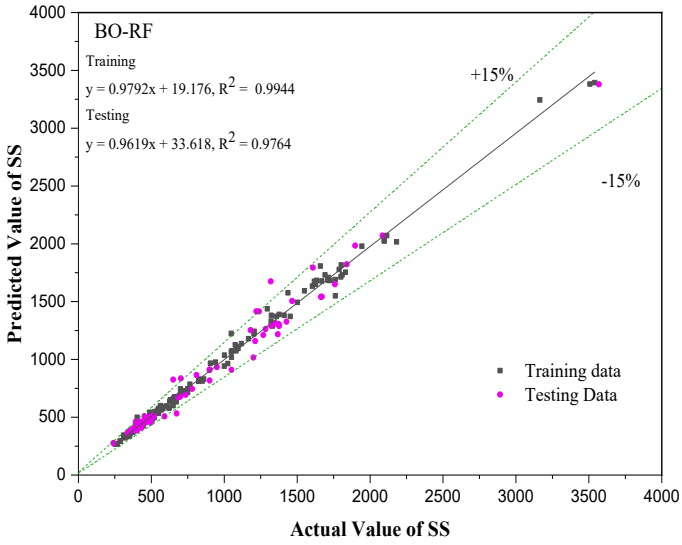
Four hybrid machine learning models (PSO-Cat, PSO-RF, BO-Cat, and BO-RF) were evaluated in terms of R^2, RMSE, MAE, and MAPE, in accordance with the evaluation criteria shown in **Fig. 4 and Table 2**. With 0.9996 for training and 0.9817 for testing, the BO-Cat model achieved the best predictive performance (R^2). With the lowest MAPE during training (1.26%), it also had the lowest RMSE (12.555 for training and 78.3947 for testing) and MAE values (8.5594 and 55.6131). The aforementioned data demonstrate their broad applicability and accuracy. The PSO-Cat model also yielded good results: the R^2 values were 0.999 (training) and 0.9874 (testing). Its error metrics were RMSE (19.6455 training, 65.0769 testing) and MAE (15.1388). Its MAPE throughout testing was 5.94%, which suggests trustworthy predictions, whereas its training and 43.3995 testing

results were both low. With somewhat lower R^2 values during testing and somewhat higher RMSE and MAE values, the RF-based models PSORF and BORF produced decent results. In particular, BORF exhibited the greatest testing error (RMSE: 88.98; MAE: 60.68). In general, PSO-Cat ranked second, after BO-Cat, as the most accurate and stable model. In contrast, the RF-based models showed somewhat worse forecast accuracy—especially throughout the testing phase.

Table 2: Performance review results of hybrid ML models

Model	Phase	R^2	RMSE	MAE	MAPE
PSO-Cat	Training	0.9999	19.6455	15.1388	2.13%
	Testing	0.9874	65.0769	43.3995	5.94%
PSO-RF	Training	0.9933	49.7676	31.2667	3.69%
	Testing	0.9789	84.2934	55.8257	6.83%
BO-Cat	Training	0.9996	12.555	8.5594	1.26%
	Testing	0.9817	78.3947	55.6131	7.13%
BO-RF	Training	0.9944	45.8405	27.8933	3.10%
	Testing	0.9764	88.9824	60.6757	7.11%





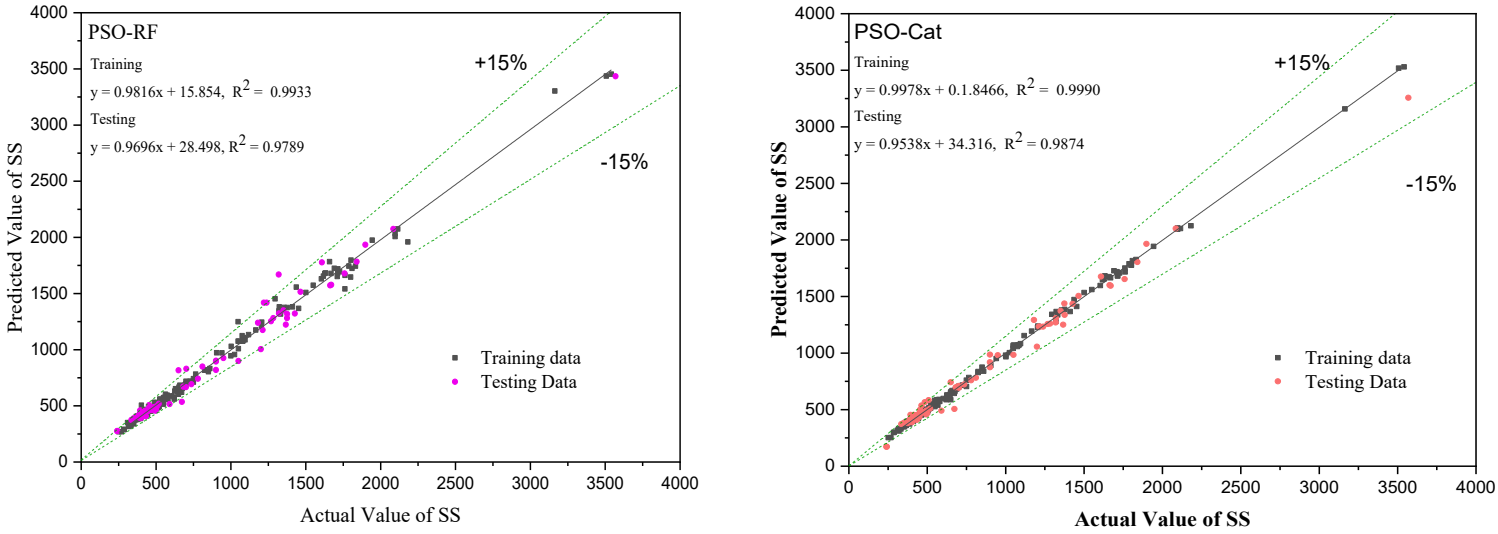


Fig. 5: Observed and predicted values (scatter plots) for the ML models

Figure 5 shows the comparison between the actual and predicted data points for the beam shear strength during both the testing and training phases. The expected results closely align with the observed shear strength values, and only a minority of the data points fell within ±15% of the predicted values. Additionally, **Figure 5** shows that almost 95% of the anticipated share strength data points, adjusted across all the models, fall within the ±15% error range, closely approximating the 1:1 linear fit line. Significantly, the BO-Cat model exhibits a strong relationship between the expected and measured values during the training phase and demonstrates good generalizability in the test phase. Symmetrically, the BO-RF regression line captures almost all of the data's variation during the training phase, indicating that it fits almost perfectly. Another hybrid model, the PSO-Cat, has a strong correlation coefficient (R^2 = 0.999) between the actual shear strength and the predicted shear strength, indicating effective results and a good predictive algorithm. PSO-RF might be an alternative approach for data-driven forecasting of shear resistance in CFSTs, and it shows higher correlation coefficients in both training and testing than other models do. The testing data correlation (R2 = 0.978) demonstrates good generalizability, which is essential for practical engineering applications. However, BO-Cat demonstrated the highest accuracy and stability, followed by PSO-Cat. In contrast, the RF-based models exhibited marginally lower prediction reliability, especially during the testing period.

Uncertainty analysis

Uncertainty assessment in machine learning applications for construction materials is important for evaluating model robustness and reliability. The performance uncertainties of the four hybrid models, namely, PSO-CatBoost, PSO-RF, BO-CatBoost, and BO-RF, at the training and test stages are shown in **Figure 6**. According to the results, the PSO-based models performed much

better than did the BO-based models. PSO-CatBoost and BO-CatBoost, in particular, had significantly lower uncertainty values, indicating greater predictability and confidence in their predictive performance across the dataset. On the other hand, PSO-RF and BO-RF had significantly higher uncertainty values, indicating that they are less stable in their predictive performance. This tendency shows that particle swarm optimization (PSO) combined with ensemble learning models such as CatBoost and random forests improves model reliability. Thus, the PSO-CatBoost and PSO-RF models become more reliable when used to predict material properties in construction-related problems.

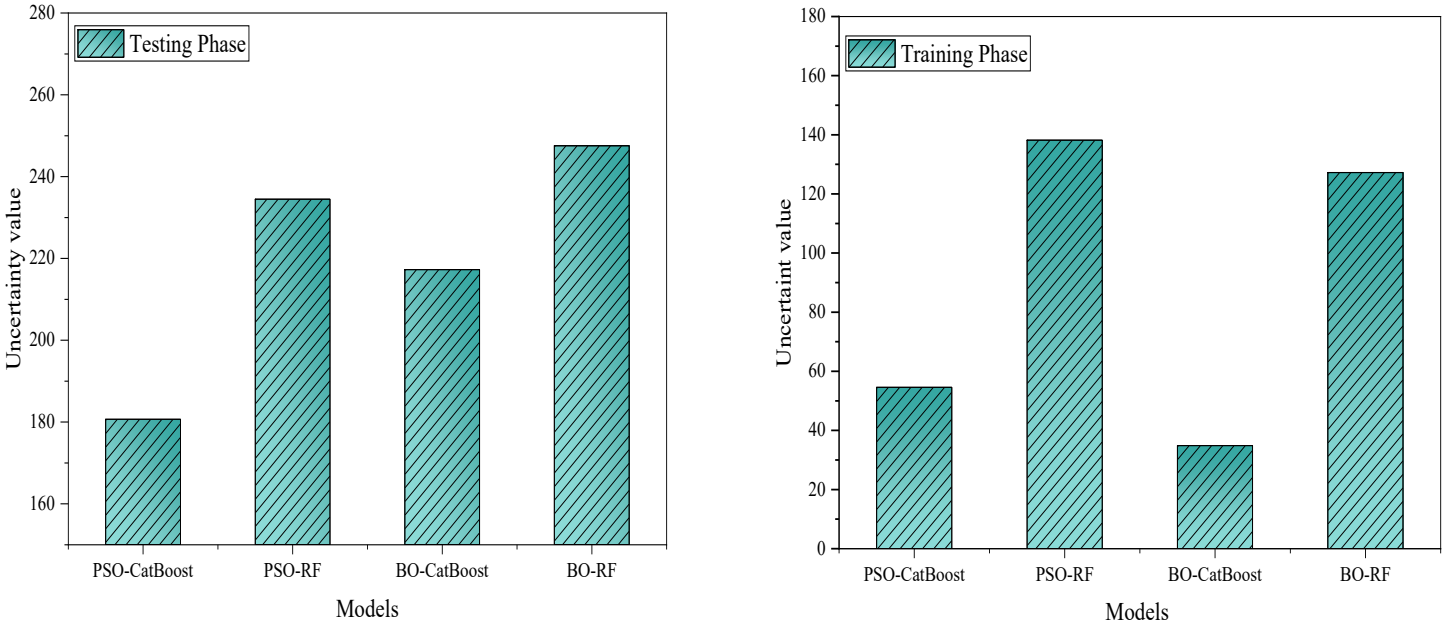


Fig. 6. Bar plots of the uncertainty analysis of the hybrid models.

4.2. SHAP Analysis

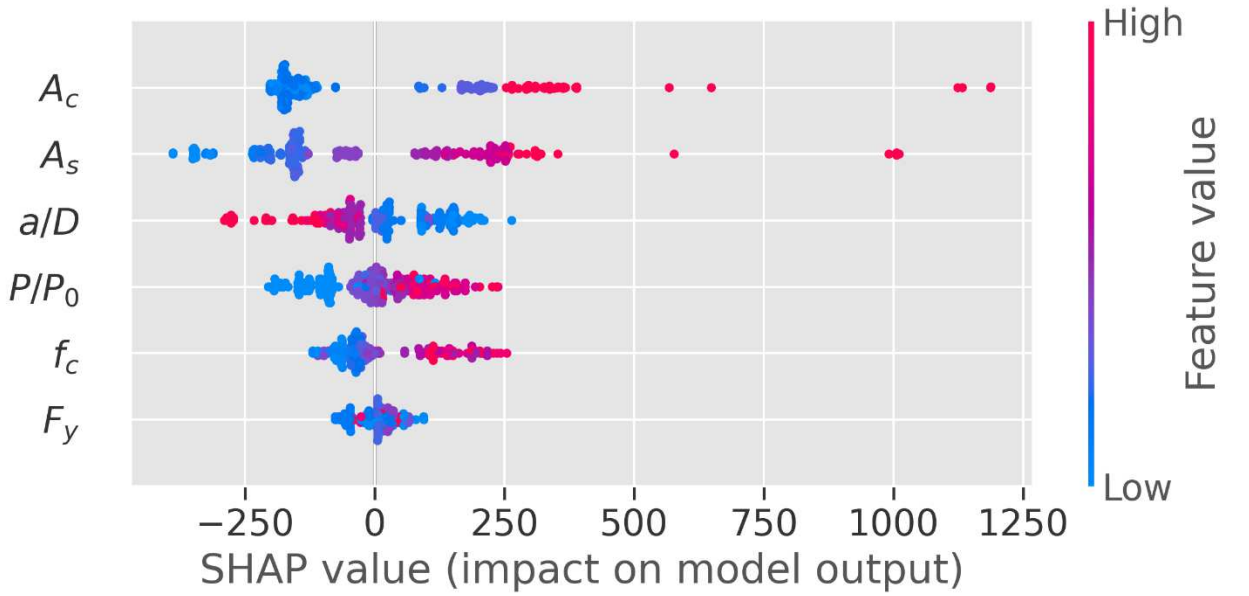


Fig. 7 Effects of SHAP impact metrics on the model outcomes for predicting shear strength.

Figure 7 SHAP summary plot illustrates how each input attribute affects the anticipated shear strength. In **Figure 7**, a dot for each dataset sample shows how a feature affects the model's prediction on the basis of its distance from the zero SHAP value. Each input feature's SHAP values are determined independently, and the dots are positioned horizontally from the zero point according to those values. A high SHAP value indicates that an input feature has a greater impact on the model's output. In contrast, a negative SHAP value indicates that the effect on the model's prediction decreases. In the figures, shades of blue indicate feature values near the lower bound, and shades of red indicate feature values near the upper bound. The concrete area (Ac) is the most significant feature in this plot; high values (indicated by red dots) significantly increase the model's predicted output, suggesting that a larger concrete cross-sectional area improves the model's load–carrying capacity or structural response. The red dots (a larger steel area) increase the forecasts, indicating that the steel reinforcement area (As) likewise has a beneficial impact. Since greater strength is usually a result of both larger concrete and reinforcing areas, this is consistent with structural engineering concepts.

There are differences in the behavior of the shear span-to-depth ratio (a/D). Since narrower shear spans typically increase shear resistance, the plot shows that low values of a/D (blue dots) are associated with positive SHAP values, suggesting that lower ratios improve the expected outcome. The mixed pattern of the normalized axial load (P/P0) suggests a more intricate, potentially nonlinear relationship; depending on how it interacts with other features, both low and high values may have different effects. Although the overall effect is less severe than that of Ac or As, the model strongly influences the concrete compressive strength (fc), with larger values marginally boosting the output. Finally, the modest trend in the steel yield strength (Fy) is similar, with higher

values resulting in a smaller but positive contribution. Overall, this SHAP analysis helps determine not only which features are most crucial but also how variations in their values affect the model's forecasts. The graphic provides transparency in the machine learning model's decision-making process while reinforcing domain-specific expertise.

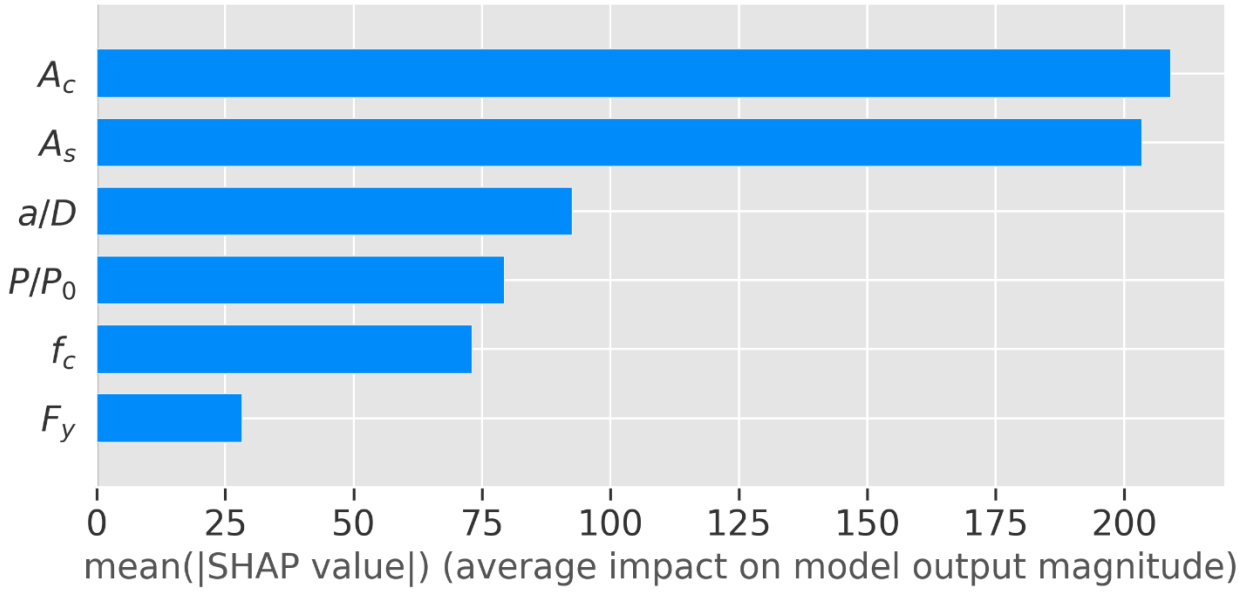


Fig. 8 Average absolute SHAP value of the significance of the shear strength feature.

The average absolute SHAP outcomes for each input feature are utilized to prioritize the significance of the SHAP features in the bar chart presented in **Figure 8,** which provides a clear picture of which factors have the largest average impact. This visualization considers only the magnitude of impact, independent of whether it raises or lowers the forecast, in contrast to the previous SHAP summary plot, which displays both the direction and value-specific influence of each feature. The SHAP feature importance bar graph shows a prioritized summary of how each input variable affects the model's output. The concrete area (Ac) has the highest mean SHAP value (just over 210) out of the six characteristics, indicating that changes in Ac have the greatest average consequence. This illustrates how important the concrete cross-section affects the structural performance. The next closest behind area is the steel reinforcement area (As), which likewise has a high SHAP value just above 200. This finding indicates that greater reinforcement significantly affects the expected output, which is again consistent with engineering knowledge that both steel and concrete areas directly affect shear strength and load capacity.

With a value of almost 90, shear span/depth (a/D) ranks third, indicating that this geometric component has a significant effect on model predictions, especially in terms of shear-dominated behavior. Similar impact values (approximately 70–80) are obtained for both the normalized axial

load (P/P0) and the concrete compressive strength (fc), indicating a minor influence on the model's assessment of the structural response. For SHAP values below 50, the steel yield strength (Fy) has the least impact on forecasts within the data range. Overall, the graphic clearly shows that sectional properties such as Ac, As, and a/D are the main factors influencing the model's predictions, whereas material strengths such as fc and Fy have a less noticeable but still significant impact.

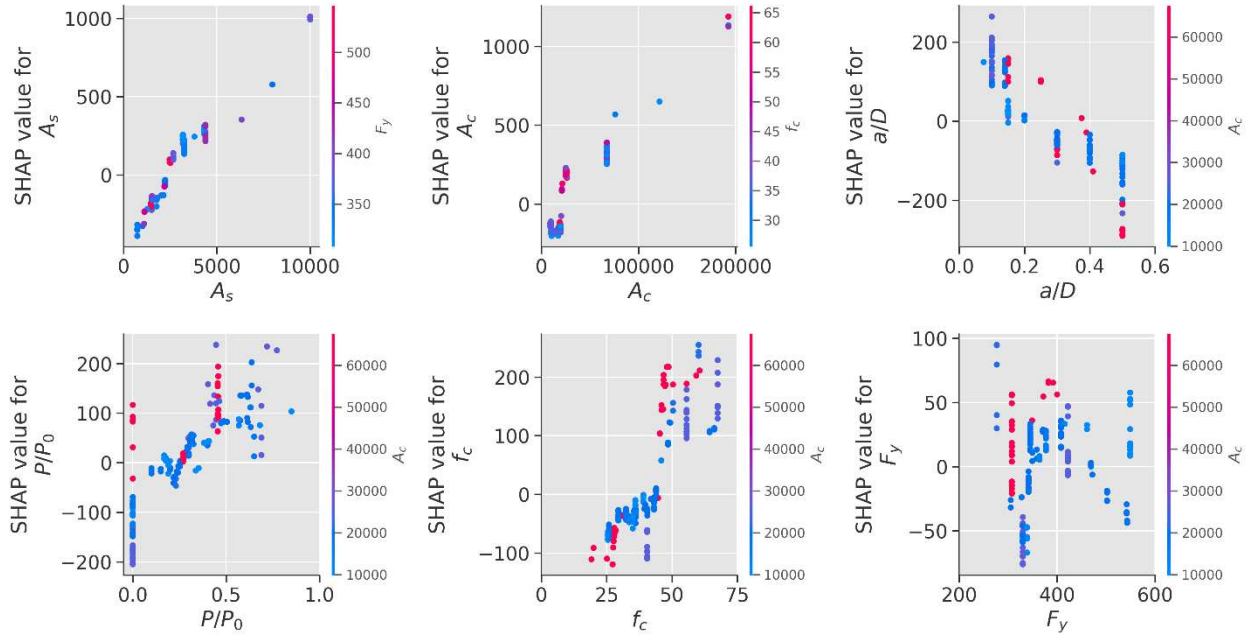


Figure 9: SHAP Dependence Graph of All Input Parameters for Shear Strength.

Figure 9 SHAP dependence plots show the true value of each attribute alongside its corresponding SHAP value, thereby highlighting its impact on the model. output and showing how individual traits influence the model's predictions. The SHAP values of variables such as the concrete area (Ac) and steel reinforcement area (As) exhibit a strong positive correlation, indicating that increases in these features consistently result in higher projected outcomes. Larger portions of steel and concrete typically result in greater strength or load-bearing capability; therefore, this aligns well with structural mechanics. These plots' color gradients show how secondary features interact. When combined with increased yield strength, the coloring of the as-plot by the steel yield strength (Fy) indicates that the reinforcement area has a greater effect on the model. Likewise, in the Ac and fc plots, significant feature interactions are observed, with the impact of compressive strength increasing with increasing concrete area.

In contrast, parameters such as the shear span-to-depth ratio (a/D) exhibit a negative association with SHAP values, meaning that better a/D ratios reduce the predicted outcome, which corresponds to how shear-critical structural segments work. Despite more unpredictability and nonlinearity, the charts for the normalized axial load (P/P0) and concrete strength (fc) generally

demonstrate positive trends. The scattered pattern in the steel yield strength (Fy) dependence graphic suggests a more complex or indirect relationship with the model's forecast. Overall, the SHAP dependence plots in **Figure 9** enhance the understanding of how the machine learning model incorporates structural factors into forecasting performance by revealing important feature interactions and confirming the dominance of geometric and sectional features such as Ac, As, and a/D.

4.3. PDP Analysis

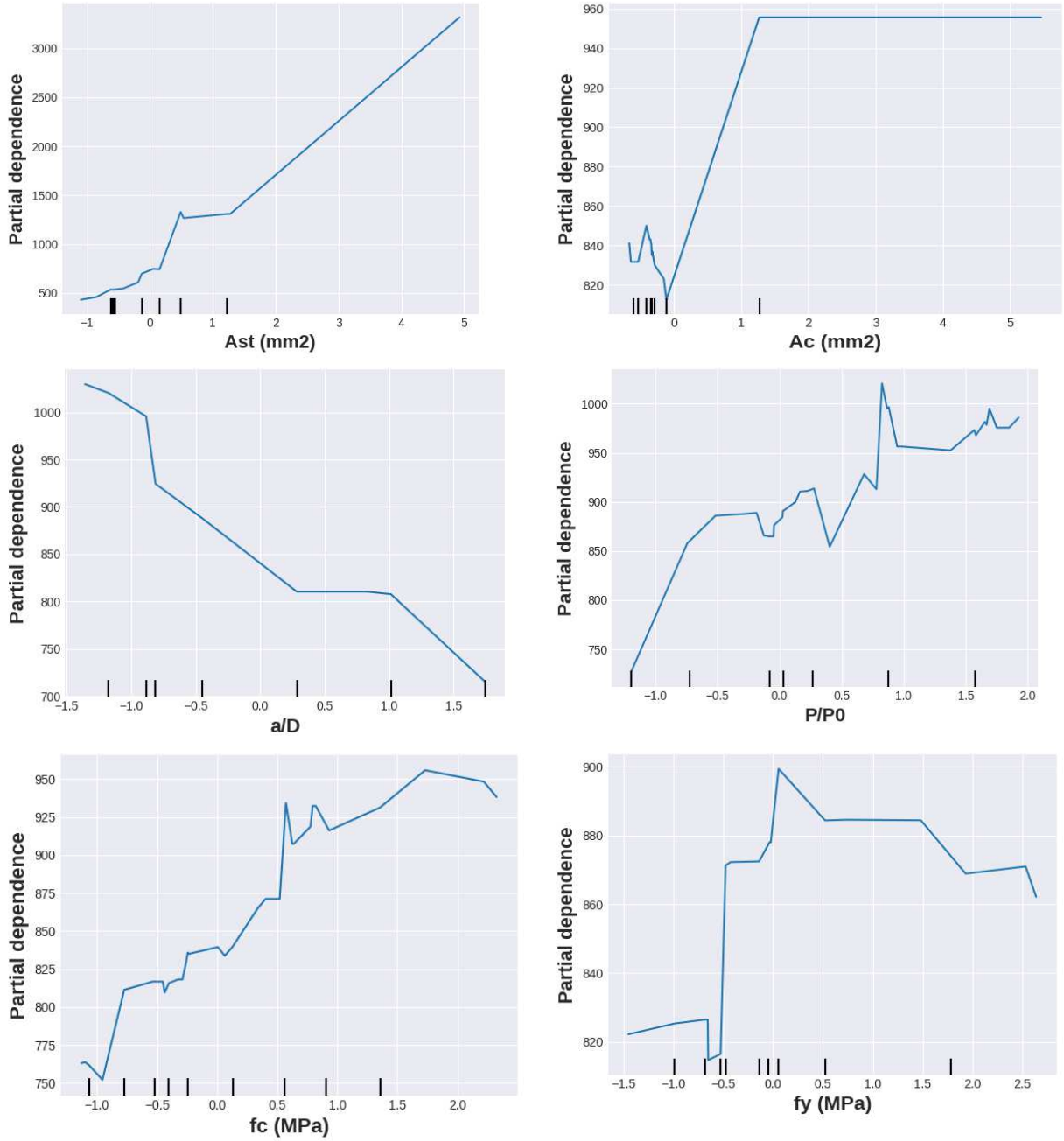


Fig. 10 PDP plots for each input parameter.

The PDP results in **Figure 10** show a clear, consistent pattern across the model. The plots revealed that the predicted shear strength increased significantly as the concrete area (Ac) increased. This demonstrated the importance of the concrete core in resisting shear forces. The steel reinforcement area (As) also had a strong positive relationship with shear strength. This means that the steel tube and concrete core work together more effectively when more steel is used, which increases the load-carrying capacity. In contrast, the shear span-to-depth ratio (a/D) had an inverse relationship with shear strength, meaning that higher values of a/D meant lower predicted strength. This trend is more consistent with that of classical structural sections, indicating that as the shear span increases, the behavior becomes more flexural-dominated, and the shear resistance decreases. The concrete compressive strength (fc) positively affects shear strength; however, the PDP curve indicates diminishing returns at elevated strength levels, suggesting that beyond a specific threshold, increases in fc have a reduced impact on shear capacity. PDP analysis was used in this study to subtract the effects of other variables and determine how individual parameters affect the predicted shear strength of circular concrete-filled steel tubes (CFSTs). To ensure that the predictions generated by metaheuristic-based machine learning algorithms are physically meaningful and consistent with known structural behavior, PDP analysis was employed primarily to provide a global interpretation of the trained models [87].

4.4. GUI Analysis

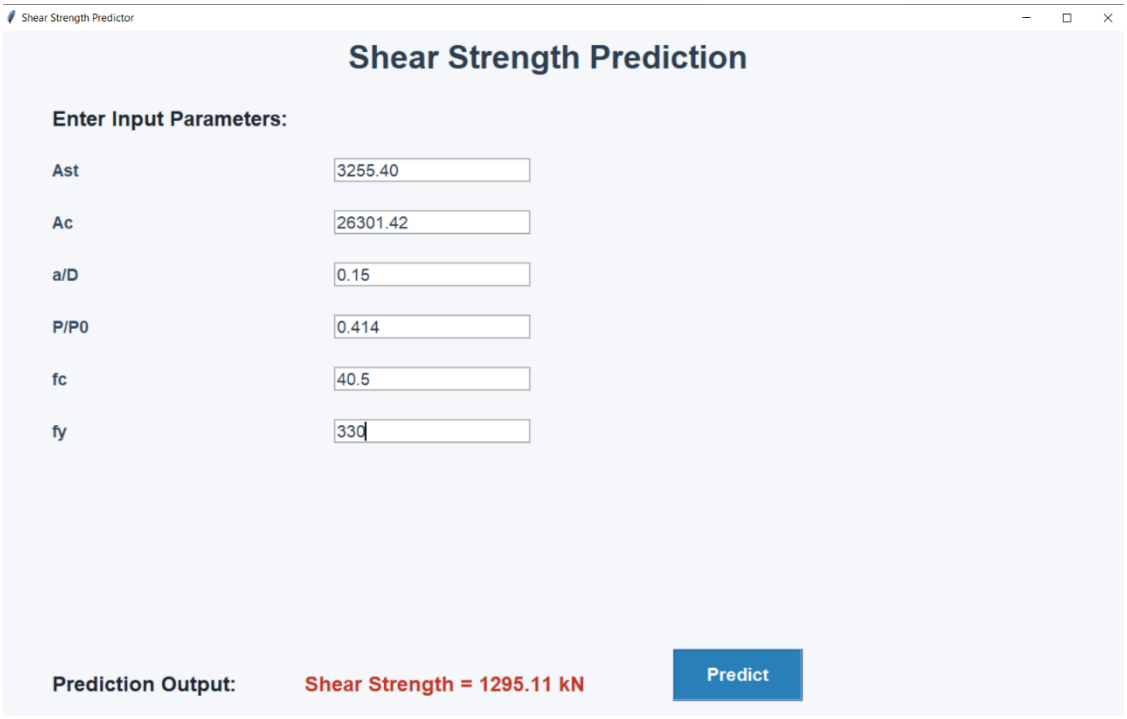


Fig. 11 GUI tool of the ML model and shear strength prediction

Figure 11. The graphical user interface (GUI), with its straightforward style, clear parameter labeling, and numerical output, makes it an invaluable tool for incorporating real-world engineering procedures. The interface, crafted with Python's Tkinter package, delivers an instant prediction when the "Predict" button is clicked, thereby removing the necessity for lengthy laboratory tests or intricate simulations. Li et al. [91] described a GUI based on sophisticated machine learning algorithms for estimating the axial load-bearing capability of RECFSTs, emphasizing user-friendly design and better prediction robustness. This study focused on six critical input parameters: Ast (tensile steel reinforcement area), Ac (concrete cross-sectional area), a/D (shear span-to-effective depth ratio), P/P0 (axial load ratio), fc (concrete compressive strength), and fy (steel yield strength). These factors represent the important geometric, material, and loading features that determine the shear behavior of a CFST. After these parameters are entered, the system calculates and displays the projected shear strength in kN. In the above scenario, the forecast is 1295.11 kN. This result provides quick feedback, assisting engineers in the constructive assessment of CFST shear strength estimation.

4.5. Compared with other research

The **Table 3** illustrate by Wahab et al. [92] compared slab–column shear strength predictions from design codes, FEA, and machine learning using data from 610 samples. The particle swarm optimization-driven feedforward neural network (PSOFNN) model was the best, with R2 =

99.37% and RMSE = 0.0275%. Using two experimental databases, Reza et al. [93] created data-based models to predict the shear strength of RC columns, both round and rectangular. The new linear regression model outperformed all the prior and nonlinear models, demonstrating the best performance. In another study that used 305 data samples, Miao et al. [94] tested three machine learning models, namely, support vector regression (SVR), back propagation neural network (BPNN), and random forest (RF), to predict the ultimate strength of circular CFSCT columns. The SVR model performed the best (R2 = 0.992), outperforming the BPNN (R2 = 0.984) and RF (R2 = 0.982) models. The shear strength of the SFRC beams was predicted via 11 machine learning models on 507 samples in a previous study[95]. Among these algorithms, XGBoost achieved the highest accuracy (85%) and the lowest RMSE and MAE. Alghossoon et al. [96] used 141 data samples and three machine learning algorithms (Gaussian processing regression, gene expression programming and nonlinear regression) to predict the shear capacity of CCFT members. GPR outperformed GEP (1.26%) and NR (1.09%) in terms of accuracy, with an average error of 0.5%. The gene expression programming (ML) algorithm was utilized in a previous study [97] to forecast the bidirectional strength of shear for columns under loads (biaxial) via an experimental database. The best GEP model achieved R2 = 0.87 for key features, significantly outperforming the ACI-318 code formulation. With the objective of developing new shear capacity formulas that outperform empirical models (R2 up to 0.975), Yu et al. [98] employed Bayesian model updating with reliability analysis on 314 data samples for circular and square CFST columns. This finding also suggests higher partial safety factors for design to ensure adequate safety. On the basis of an experimental dataset derived from the literature, Cakiroglu et al. [99] created ML models to predict the shear strength of reinforced concrete beams. XGBoost outperformed code equations and achieved the highest accuracy (R2 = 0.94); the effects of influential features, model accuracy, and SHAP-based features were examined. Wakjira et al. [100] used reliability analysis to calibrate resistance-reduction factors for target reliability and developed a machine learning algorithm to predict the shear capacity of reinforced concrete beams with inorganic composites. XGBoost outperformed existing models in terms of accuracy, safety, and economic performance.

Table 3. Shear strength prediction results from previous research

SI No.	Specimen Type	Number of Data	ML Algorithms Used	Best Performing ML Model	Predicted Output	Evaluation Parameter		Reference
						R^2 Value	RMSE Value	
1.	Circular Concrete-Filled Steel Tubes (CFSTs)	230	Particle Swarm Optimization-Category Boosting (PSO-Cat), Particle Swarm Optimization-Random Forest (PSO-RF), and Bayesian Optimization-Category Boosting (BO-Cat), Bayesian Optimization-Random Forest (BO-RF)	Bayesian Optimization-Category Boosting (BO-Cat)	Shear Strength	0.999	19.6455	Present Study
2.	Slab–Column Connections	610	Particle swarm optimization-based FNN (PSOFNN), Bat algorithm-based FNN (BATFNN) and Feed FNN	Particle swarm optimization-based feedforward neural network (PSOFNN)	Shear Strength	99.37%	-	[92]
3.	Rectangular and Circular Reinforced Concrete Columns	325 & 172	Shear Strength Model (SSM)	Shear Strength Model (SSM)	Shear Strength	0.942	-	[93]
4.	Circular Concrete-Filled Fiber-Reinforced Polymer–Steel Composite Tube Columns	305	SVR, RF and Back Propagation Neural Network (BPNN)	Support vector regression (SVR)	Ultimate Strength	0.992	-	[94]
5.	RC Columns	74	Linear Regression (LRegr), Nonlinear Regression (NLRegr) and Extreme Gradient Boosting (XGBoost)	Extreme Gradient Boosting (XGBoost)	Shear Strength	99.65%		[101]
6.	Steel Fiber RC Beams	507	DT, RF, SVM, KNN, ANN, LR, CatBoost, XGBoost, and AdaBoost	XGBoost	Shear Strength	0.739	1.346	[95]
7.	Circular Concrete-Filled Tube (CCFT)	141	Gene Expression Programming (GEP), Gaussian Processing Regression (GPR), and Nonlinear Regression (NR)	Gaussian Processing Regression (GPR)	Shear Strength	0.99	-	[96]
8.	RC Columns	47	Gene Expression Programming (GEP)	(GEP)	Bidirecti-onal Shear Strength	0.87	-	[97]
9.	Circular and Square Concrete-	314	Bayesian Model	Bayesian Model	Shear Strength	0.975	-	[98]

	Filled Steel Tubes							
10.	RC Beam	128	Ensemble Learning Methods	XGBoost	Shear Strength	0.94		[99]
11.	RC Beam	173	SVR, RF, DT, Extremely Randomized Trees, Gradient Tree Boosting, and (XGBoost)	(XGBoost)	Shear Capacity	0.995	10.96	[100]

5.0 Conclusion

In this work, metaheuristic optimization-based machine learning models were applied to estimate the shear strength of circular concrete-filled steel tubes (CFSTs). By integrating particle swarm optimization (PSO) and Bayesian optimization (BO) with random forest (RF) and category boosting (Cat), highly accurate predictive frameworks have been developed. A total of six input variables were considered, with 270 data samples for shear strength prediction, all sourced from previous studies, and hyperparameter optimization grid search techniques were carried out. Seventy percent of these resources were meant for training, whereas thirty percent were meant for testing. Among the models, PSO-Cat and BO-Cat achieved superior performance, demonstrating excellent generalizability across the training and testing phases, with R^2 values exceeding 0.98. These findings confirm that shear strength prediction is essential for ensuring both safety and efficiency in CFST design, where abrupt shear failure poses significant structural risks. Furthermore, Shapley additive explanations (SHAPs), partial dependence plots (PDPs), and a graphical user interface (GUI) were used to analyze the contributions and interactions of the input materials to shear strength prediction. Four evaluation criteria were subsequently used to check how well the models worked and how accurate they were. Based on these results, the following conclusions were drawn:

- From the correlation analysis, the input parameter shows the strongest positive correlation with the shear strength prediction (CFST) of the cross-sectional area of the steel tube Ast (0.90) and the concrete core Ac (0.81). Conversely, the yield stress of steel, Fy (-0.22), and the ratio of the shear span length to the cross-sectional diameter, a/D (-0.13), have weak negative correlations with the shear strength.

- The four hybrid ML techniques showed great performance and strong generalizability; therefore, they are quite reliable for forecasting the STs of circular concrete-filled steel tubes (CFSTs). All the models had R^2 values exceeding 0.99 during training and approximately 0.98 during testing, illustrating their robustness and accuracy in prediction.

- With the highest R^2 of 0.9817, the BO-cat model showed better precision and consistency in predicting the shear strength of CFSTs. Its great predictive performance and generalizability are shown by its lowest RMSE (88.9824), MAE (60.6757), and MAPE

(7.11%). The PSO-Cat model also performed well, with an R^2 of 0.9874, an RMSE of 65.0767, an MAE of 43.3995, and a MAPE of 5.94%. These results suggest that while both models work, the BO-Cat model is the most reliable; the PSO-Cat model closely follows.

- SHAP and PDP analyses provided transparent interpretability, revealing that the concrete area (Ac), steel reinforcement area (As), and shear span-to-depth ratio (a/D) are the dominant factors influencing the shear capacity. In contrast, the concrete compressive strength (fc) and steel yield strength (Fy) have minimal influences. This interpretability not only validates the models' physical relevance but also enhances confidence in their application.

- To further integrate these advanced prediction models into a practical engineering tool, a graphical user interface (GUI) was created, allowing designers to estimate shear strength openly, honestly, and accurately.

5.1 Limitations and Future Studies

This research delivers a reliable, user-friendly framework that outperforms conventional empirical methods, offering significant potential to advance CFST design practices. Future research should aim to expand the database by incorporating large-scale experimental and field data to improve the generalizability of the models. Additional structural parameters, including bond–slip effects, axial loading interactions, and varying boundary conditions, should be considered to capture more complex behaviors. Extending the framework to other CFST geometries and loading scenarios (e.g., combined shear and bending, cyclic or seismic loading) would further enhance its applicability. Moreover, integrating physics-informed machine learning approaches and deep learning algorithms could help embed fundamental mechanics into the predictive process, improving both accuracy and reliability. Finally, enhancing the GUI to support real-time parametric analysis and code-based design checks could maximize its utility for practicing engineers.

Credit authorship contribution statement

Sourov Paul: Conceptualization, Formal analysis, Methodology, Software, Writing – original draft, Writing – review & editing. **Pobithra Das:** Writing – review & editing, Resources, Software, Formal analysis. **Md Khaled Ahmed:** Writing – original draft, Resources, Data curation, Methodology. **Asmaul Husna Chara:** Resources, Data curation, Writing – original draft. **Abul Kashem:** Writing – review & editing, Writing – original draft, Data curation, Formal analysis, Software, Conceptualization. **Mahmudul Haque Jamil:** Methodology, Data curation, Writing – original draft. **Hafiz Farooq Ahmed:** Data curation, Writing – review & editing, **Md Ehtesamul Haque:** Writing – review & editing, Resources, Conceptualization. **Rama Samy Naidu:** Writing – original draft, Writing – review & editing, Resources. **Ammar Fayez Alshayeb:** Writing – review & editing, Resources, Conceptualization. **Ziad Shatnawi:** Writing – review & editing, Resources, Conceptualization. **Muhammad Imran Khan:** Conceptualization, Writing – review & editing. **Abdulrahman Fahad Alfuhaid:** Writing – original draft, Writing – review & editing, **Md Arifuzzaman:** Supervision, Writing – review & editing, Resources, Conceptualization, Funding acquisition.

Funding: This work was supported by the Deanship of Scientific Research, Vice Presidency for Graduate Studies and Scientific Research, King Faisal University, Saudi Arabia [Grant No. KFU263579].

Data Availability Statement:

The datasets utilised during the current study are available on GitHub.

(https://github.com/Sourov-120/ML-Models-for-Predicting-Shear-Strength-of-Circular-CFST-with-SHAP-Based-and-PDP-Interpretability-)

Acknowledgments: This work was supported by the Deanship of Scientific Research, Vice Presidency for Graduate Studies and Scientific Research, King Faisal University, Saudi Arabia [Grant No. KFU263579].

Conflicts of interest: The authors declare that they have no conflicts of interest.

Reference

[1] Y. Yu, W. Wu, J. Yan, J. Zang, Probabilistic models for shear strength of circular and square concrete-filled steel tubes, AIP Adv 15 (2025). https://doi.org/10.1063/5.0250829.

[2] M.-Z. Zhao, D.E. Lehman, X. Zhang, C.W. Roeder, Evaluation and improvement of shear–strength expressions for circular concrete-filled steel tubes, Journal of Structural Engineering & Applied Mechanics 6 (2023). https://doi.org/10.31462/jseam.2023.02167194.

[3] W.-D. Wang, Z.-L. Jia, Y.-L. Shi, E.L. Tan, Performance of steel-reinforced circular concrete-filled steel tubular members under combined compression and torsion, J Constr Steel Res 173 (2020) 106271. https://doi.org/10.1016/j.jcsr.2020.106271.

[4] L.-H. Han, W. Li, Seismic Performance of Concrete-Filled Steel Tubular (CFST) Structures, in: Seismic Design of Industrial Facilities, Springer Fachmedien Wiesbaden, 2014: pp. 361–368. https://doi.org/10.1007/978-3-658-02810-7_30.

[5] H. Kenarangi, M. Bruneau, Shear Strength of Composite Circular Reinforced Concrete–Filled Steel Tubes, Journal of Structural Engineering 146 (2020). https://doi.org/10.1061/(asce)st.1943-541x.0002456.

[6] X.L. Zhao, J.A. Packer, Tests and design of concrete-filled elliptical hollow section stub columns, Thin-Walled Structures 47 (2009) 617–628. https://doi.org/10.1016/j.tws.2008.11.004.

[7] D. V Rosato, Plastics Engineered Product Design, 2003.

[8] Standard Test Method for Shear Strength of Plastics by Punch Tool, (2024).

[9] N. Anwar, F. Najam, Response and Design for Shear and Torsion, in: 2017: pp. 251–328. https://doi.org/10.1016/B978-0-12-804443-8.00004-X.

[10] Z. Lai, A.H. Varma, Noncompact and slender circular CFT members: Experimental database, analysis, and design, J Constr Steel Res 106 (2015) 220–233. https://doi.org/10.1016/J.JCSR.2014.11.005.

[11] Z. Lai, A.H. Varma, K. Zhang, Noncompact and slender rectangular CFT members: Experimental database, analysis, and design, J Constr Steel Res 101 (2014) 455–468. https://doi.org/10.1016/j.jcsr.2014.06.004.

[12] Y. Ye, L.H. Han, Z. Tao, S.L. Guo, Experimental behavior of concrete-filled steel tubular members under lateral shear loads, J Constr Steel Res 122 (2016) 226–237. https://doi.org/10.1016/j.jcsr.2016.03.012.

[13] C. Xu, L. Haixiao, H. Chengkui, Experimental study on shear resistance of self-stressing concrete filled circular steel tubes, J Constr Steel Res 65 (2009) 801–807. https://doi.org/10.1016/j.jcsr.2008.12.004.

[14] N. Raveendran, G.R. Babu, A critical review on using concrete filled steel tubular column with artificial damage scenario, in: 2023: p. 040013. https://doi.org/10.1063/5.0165740.

[15] Z. Lai, A.M. Asce, A.H. Varma, M. Asce, High-Strength Rectangular CFT Members: Database, Modeling, and Design of Short Columns Introduction and Background, (2018). https://doi.org/10.1061/(ASCE)ST.1943.

[16] J. Wei, X. Luo, Z. Lai, A.H. Varma, Experimental Behavior and Design of High-Strength Circular Concrete-Filled Steel Tube Short Columns, Journal of Structural Engineering 146 (2020). https://doi.org/10.1061/(asce)st.1943-541x.0002474.

[17] Y. Wang, H. Lin, Z. Lai, D. Li, weisheng zhou, X. Yang, Flexural Behavior of High-Strength Rectangular Concrete-Filled Steel Tube Members, Journal of Structural Engineering 148 (2022) 4021230. https://doi.org/10.1061/(ASCE)ST.1943-541X.0003192.

[18] L. Lowes, C.B. Coughlin, P. Lundeen, L.N. Lowes, D.E. Lehman, Recommendations for Modeling the Nonlinear Response of Slender Reinforced Concrete Walls Using PERFORM-3D, 2018. www.csiamerica.com.

[19] A. Alghossoon, A. Tarawneh, G. Almasabha, Y. Murad, E. Saleh, H.A. yahia, A.A. yahya, H. Sahawneh, Shear strength of circular concrete-filled tube (CCFT) members using human-guided artificial intelligence approach, Eng Struct 282 (2023) 115820. https://doi.org/10.1016/J.ENGSTRUCT.2023.115820.

[20] AASHTO LRFD Bridge Design Specification, 2007.

[21] R. Johnson, D. Anderson, EN1994 Eurocode 4: Design of composite steel and concrete structures, Proceedings of The Institution of Civil Engineers-Civil Engineering - PROC INST CIVIL ENG-CIVIL ENG 144 (2001) 33–38. https://doi.org/10.1680/cien.2001.144.6.33.

[22] W. Bridge Office, Bridge Design Manual (LRFD) Engineering and Regional Operations Bridge and Structures Office, 2024.

[23] X.-X. Zha, S.-T. Zhong, The introduction of “technical specification of solid and hollow concrete-filled steel tubular structures,” 43 (2011) 1–6.

[24] C. Xiao, S. Cai, T. Chen, C. Xu, Experimental study on shear capacity of circular concrete filled steel tubes, Steel and Composite Structures 13 (2012). https://doi.org/10.12989/scs.2012.13.5.437.

[25] C. Roeder, D. Lehman, A. Heid, T. Maki, Shear Design Expressions for Concrete Filled Steel Tube and Reinforced Concrete Filled Tube Components, 2016.

[26] T.-T. Le, Practical Hybrid Machine Learning Approach for Estimation of Ultimate Load of Elliptical Concrete-Filled Steel Tubular Columns under Axial Loading, Advances in Civil Engineering (2020). https://doi.org/10.1155/2020/8832522.

[27] H.S. Mohamed, T. Qiong, H.F. Isleem, R.K. Tipu, R.I. Shahin, S.A. Yehia, P. Jangir, Arpita, M. Khishe, Compressive behavior of elliptical concrete-filled steel tubular short columns using numerical investigation and machine learning techniques, Sci Rep 14 (2024) 27007. https://doi.org/10.1038/s41598-024-77396-5.

[28] F. Lyu, X. Fan, F.-X. Ding, Z. Chen, Prediction of the Axial Compressive Strength of Circular Concrete-Filled Steel Tube Columns using Sine Cosine Algorithm-Support Vector Regression, Compos Struct 273 (2021) 114282. https://doi.org/10.1016/j.compstruct.2021.114282.

[29] A. Albidah, Y. Abbas, Improving Shear Strength Prediction in Steel Fiber Reinforced Concrete Beams: Stacked Ensemble Machine Learning Modeling and Practical Applications, Buildings 14 (2024) 2169. https://doi.org/10.3390/buildings14072169.

[30] W. Ben Chaabene, M. Flah, M.L. Nehdi, Machine learning prediction of mechanical properties of concrete: Critical review, Constr Build Mater 260 (2020). https://doi.org/10.1016/j.conbuildmat.2020.119889.

[31] A. Pal, K.S. Ahmed, F.Z. Hossain, M.S. Alam, Machine learning models for predicting compressive strength of fiber-reinforced concrete containing waste rubber and recycled aggregate, J Clean Prod 423 (2023). https://doi.org/10.1016/j.jclepro.2023.138673.

[32] P. Li, M. Ali Khan, M.G. Ahmed, H. Hassan Awan, A. Zafar, M. Faisal Javed, M. Ijaz Khan, S. Qayyum, M.Y. Malik, F. Wang, Sustainable use of chemically modified tyre rubber in concrete: Machine learning based novel predictive model, Chem Phys Lett 793 (2022). https://doi.org/10.1016/j.cplett.2022.139478.

[33] A. Gregori, C. Castoro, G. Venkiteela, Predicting the compressive strength of rubberized concrete using artificial intelligence methods, Sustainability (Switzerland) 13 (2021). https://doi.org/10.3390/su13147729.

[34] X. Huang, J. Zhang, J. Sresakoolchai, S. Kaewunruen, Machine learning aided design and prediction of environmentally friendly rubberized concrete, Sustainability (Switzerland) 13 (2021) 1–27. https://doi.org/10.3390/su13041691.

[35] M. Kovačević, S. Lozančić, E.K. Nyarko, M. Hadzima-nyarko, Modeling of compressive strength of self-compacting rubberized concrete using machine learning, Materials 14 (2021). https://doi.org/10.3390/ma14154346.

[36] M.C. Kang, D.Y. Yoo, R. Gupta, Machine learning-based prediction for compressive and flexural strengths of steel fiber-reinforced concrete, Constr Build Mater 266 (2021). https://doi.org/10.1016/j.conbuildmat.2020.121117.

[37] S. Zakir Sarothi, K. Sakil Ahmed, N. Imtiaz Khan, A. Ahmed, M.L. Nehdi, Predicting bearing capacity of double shear bolted connections using machine learning, Eng Struct 251 (2022). https://doi.org/10.1016/j.engstruct.2021.113497.

[38] S. Zakir Sarothi, K. Sakil Ahmed, N. Imtiaz Khan, A. Ahmed, M.L. Nehdi, Machine learning-based failure mode identification of double shear bolted connections in structural steel, Eng Fail Anal 139 (2022). https://doi.org/10.1016/j.engfailanal.2022.106471.

[39] K. Demertzis, K. Kostinakis, K. Morfidis, L. Iliadis, An interpretable machine learning method for the prediction of R/C buildings' seismic response, Journal of Building Engineering 63 (2023). https://doi.org/10.1016/j.jobe.2022.105493.

[40] S. Mangalathu, H. Jang, S.H. Hwang, J.S. Jeon, Data-driven machine-learning-based seismic failure mode identification of reinforced concrete shear walls, Eng Struct 208 (2020). https://doi.org/10.1016/j.engstruct.2020.110331.

[41] C. Cakiroglu, K. Islam, G. Bekdaş, U. Isikdag, S. Mangalathu, Explainable machine learning models for predicting the axial compression capacity of concrete filled steel tubular columns, Constr Build Mater 356 (2022). https://doi.org/10.1016/j.conbuildmat.2022.129227.

[42] M.F. Javed, F. Farooq, S.A. Memon, A. Akbar, M.A. Khan, F. Aslam, R. Alyousef, H. Alabduljabbar, S.K. Ur Rehman, New prediction model for the ultimate axial capacity of concrete-filled steel tubes: An evolutionary approach, Crystals (Basel) 10 (2020) 1–33. https://doi.org/10.3390/cryst10090741.

[43] A.I. Nour, E.M. Güneyisi, Prediction model on compressive strength of recycled aggregate concrete filled steel tube columns, Compos B Eng 173 (2019). https://doi.org/10.1016/j.compositesb.2019.106938.

[44] T.T. Le, P.G. Asteris, M.E. Lemonis, Prediction of axial load capacity of rectangular concrete-filled steel tube columns using machine learning techniques, Eng Comput 38 (2022) 3283–3316. https://doi.org/10.1007/s00366-021-01461-0.

[45] M. Ahmadi, H. Naderpour, A. Kheyroddin, ANN Model for Predicting the Compressive Strength of Circular Steel-Confined Concrete, International Journal of Civil Engineering 15 (2017) 213–221. https://doi.org/10.1007/s40999-016-0096-0.

[46] A. Bardhan, R. Biswas, N. Kardani, M. Iqbal, P. Samui, M.P. Singh, P.G. Asteris, A novel integrated approach of augmented gray wolf optimizer and ANN for estimating axial load carrying-capacity of concrete-filled steel tube columns, Constr Build Mater 337 (2022). https://doi.org/10.1016/j.conbuildmat.2022.127454.

[47] C. Deng, X. Xue, L. Tao, Prediction of ultimate bearing capacity of concrete filled steel tube stub columns via machine learning, Soft Comput 28 (2024) 5953–5967. https://doi.org/10.1007/s00500-023-09343-x.

[48] A. Alghossoon, A. Tarawneh, G. Almasabha, Y. Murad, E. Saleh, H.A. yahia, A.A. yahya, H. Sahawneh, Shear strength of circular concrete-filled tube (CCFT) members using human-guided artificial intelligence approach, Eng Struct 282 (2023). https://doi.org/10.1016/j.engstruct.2023.115820.

[49] A. Mansouri, M. Mansouri, S. Mangalathu, Interpretable machine learning model for shear strength estimation of circular concrete-filled steel tubes, Structural Design of Tall and Special Buildings 33 (2024). https://doi.org/10.1002/tal.2111.

[50] Y. Yu, W. Wu, J. Yan, J. Zang, Probabilistic models for shear strength of circular and square concrete-filled steel tubes, AIP Adv 15 (2025). https://doi.org/10.1063/5.0250829.

[51] C. Xu, L. Haixiao, H. Chengkui, Experimental study on shear resistance of self-stressing concrete filled circular steel tubes, J Constr Steel Res 65 (2009) 801–807. https://doi.org/10.1016/j.jcsr.2008.12.004.

[52] D. Lehman, C. Roeder, A. Heid, T. Maki, B. Khaleghi, Shear response of concrete filled tubes part 1: Experiments, J Constr Steel Res 150 (2018) 528–540. https://doi.org/10.1016/j.jcsr.2018.08.027.

[53] A. Mansouri, M. Mansouri, S. Mangalathu, Interpretable machine learning model for shear strength estimation of circular concrete-filled steel tubes, The Structural Design of Tall and Special Buildings 33 (2024). https://doi.org/10.1002/tal.2111.

[54] H. Kenarangi, M. Bruneau, Investigation of Cyclic-Shear Behavior of Circular-Reinforced Concrete-Filled Steel Tubes, Journal of Structural Engineering 146 (2020). https://doi.org/10.1061/(ASCE)ST.1943-541X.0002598.

[55] S. Li, Z. Liu, Y. Lu, T. Zhu, Shear performance of steel fibers reinforced self-confinement and self-compacting concrete-filled steel tube stub columns, Constr Build Mater 147 (2017) 758–775. https://doi.org/10.1016/j.conbuildmat.2017.04.192.

[56] Z. Liu, Y. Lu, S. Li, J. Liao, Shear response of steel fiber reinforced recycled concrete-filled steel tube columns, Advances in Structural Engineering 24 (2021) 2684–2704. https://doi.org/10.1177/13694332211009322.

[57] Z.-C. Yang, L.-H. Han, C. Hou, Performance of recycled aggregate concrete-filled steel tubular columns under combined compression and shear load, Eng Struct 253 (2022) 113771. https://doi.org/10.1016/j.engstruct.2021.113771.

[58] J.T. Hancock, T.M. Khoshgoftaar, CatBoost for big data: an interdisciplinary review, J Big Data 7 (2020). https://doi.org/10.1186/s40537-020-00369-8.

[59] G. Huang, L. Wu, X. Ma, W. Zhang, J. Fan, X. Yu, W. Zeng, H. Zhou, Evaluation of CatBoost method for prediction of reference evapotranspiration in humid regions, J Hydrol (Amst) 574 (2019) 1029–1041. https://doi.org/10.1016/j.jhydrol.2019.04.085.

[60] S. Ben Jabeur, C. Gharib, S. Mefteh-Wali, W. Ben Arfi, CatBoost model and artificial intelligence techniques for corporate failure prediction, Technol Forecast Soc Change 166 (2021). https://doi.org/10.1016/j.techfore.2021.120658.

[61] M. Luo, Y. Wang, Y. Xie, L. Zhou, J. Qiao, S. Qiu, Y. Sun, Combination of feature selection and catboost for prediction: The first application to the estimation of aboveground biomass, Forests 12 (2021) 1–22. https://doi.org/10.3390/f12020216.

[62] W. Chang, X. Wang, J. Yang, T. Qin, An Improved CatBoost-Based Classification Model for Ecological Suitability of Blueberries, Sensors 23 (2023). https://doi.org/10.3390/s23041811.

[63] Z. El Mrabet, N. Sugunaraj, P. Ranganathan, S. Abhyankar, Random Forest Regressor-Based Approach for Detecting Fault Location and Duration in Power Systems, Sensors 22 (2022). https://doi.org/10.3390/s22020458.

[64] U. Grömping, Variable importance assessment in regression: Linear regression versus random forest, American Statistician 63 (2009) 308–319. https://doi.org/10.1198/tast.2009.08199.

[65] G. Biau, G.B. Fr, Analysis of a Random Forests Model, 2012.

[66] J.L. Speiser, M.E. Miller, J. Tooze, E. Ip, A comparison of random forest variable selection methods for classification prediction modeling, Expert Syst Appl 134 (2019) 93–101. https://doi.org/10.1016/j.eswa.2019.05.028.

[67] W. Chen, X. Xie, J. Wang, B. Pradhan, H. Hong, D.T. Bui, Z. Duan, J. Ma, A comparative study of logistic model tree, random forest, and classification and regression tree models for spatial prediction of landslide susceptibility, Catena (Amst) 151 (2017) 147–160. https://doi.org/10.1016/j.catena.2016.11.032.

[68] J.L. Speiser, M.E. Miller, J. Tooze, E. Ip, A comparison of random forest variable selection methods for classification prediction modeling, Expert Syst Appl 134 (2019) 93–101. https://doi.org/10.1016/j.eswa.2019.05.028.

[69] S. Gaur, B.R. Chahar, D. Graillot, Analytic elements method and particle swarm optimization based simulation-optimization model for groundwater management, J Hydrol (Amst) 402 (2011) 217–227. https://doi.org/10.1016/j.jhydrol.2011.03.016.

[70] D. Wang, D. Tan, L. Liu, Particle swarm optimization algorithm: an overview, Soft Comput 22 (2018) 387–408. https://doi.org/10.1007/s00500-016-2474-6.

[71] Y. Zhang, S. Wang, G. Ji, A Comprehensive Survey on Particle Swarm Optimization Algorithm and Its Applications, Math Probl Eng 2015 (2015). https://doi.org/10.1155/2015/931256.

[72] Y. Jiang, T. Hu, C.C. Huang, X. Wu, An improved particle swarm optimization algorithm, Appl Math Comput 193 (2007) 231–239. https://doi.org/10.1016/j.amc.2007.03.047.

[73] A. Banks, J. Vincent, C. Anyakoha, A review of particle swarm optimization. Part I: Background and development, Nat Comput 6 (2007) 467–484. https://doi.org/10.1007/s11047-007-9049-5.

[74] H. Jair Escalante, M. Montes, L. Enrique Sucar ESUCAR, Particle Swarm Model Selection, 2009.

[75] H.M. Torun, M. Swaminathan, A. Kavungal Davis, M.L.F. Bellaredj, A Global Bayesian Optimization Algorithm and Its Application to Integrated System Design, IEEE Trans Very Large Scale Integr VLSI Syst 26 (2018) 792–802. https://doi.org/10.1109/TVLSI.2017.2784783.

[76] X. Wang, Y. Jin, S. Schmitt, M. Olhofer, Recent Advances in Bayesian Optimization, ACM Comput Surv 55 (2023). https://doi.org/10.1145/3582078.

[77] C.F. Lima, F.G. Lobo, M. Pelikan, D.E. Goldberg, Model accuracy in the Bayesian optimization algorithm, Soft Comput 15 (2011) 1351–1371. https://doi.org/10.1007/s00500-010-0675-y.

[78] B. Shahriari, K. Swersky, Z. Wang, R.P. Adams, N. De Freitas, Taking the human out of the loop: A review of Bayesian optimization, Proceedings of the IEEE 104 (2016) 148–175. https://doi.org/10.1109/JPROC.2015.2494218.

[79] J. Wu, X.Y. Chen, H. Zhang, L.D. Xiong, H. Lei, S.H. Deng, Hyperparameter optimization for machine learning models based on Bayesian optimization, Journal of Electronic Science and Technology 17 (2019) 26–40. https://doi.org/10.11989/JEST.1674-862X.80904120.

[80] D.-C. Feng, A.M. Asce, W.-J. Wang, S. Mangalathu, E. Taciroglu, M. Asce, Interpretable XGBoost-SHAP Machine-Learning Model for Shear Strength Prediction of Squat RC Walls, (2021). https://doi.org/10.1061/(ASCE).

[81] A.S. Antonini, J. Tanzola, L. Asiain, G.R. Ferracutti, S.M. Castro, E.A. Bjerg, M.L. Ganuza, Machine Learning model interpretability using SHAP values: Application to Igneous Rock Classification task, Applied Computing and Geosciences 23 (2024). https://doi.org/10.1016/j.acags.2024.100178.

[82] M.H. Jamil, R. Jagirdar, A. Kashem, M.N. Ali, D. Deb, Modeling of Marshall Stability of plastic-reinforced asphalt concrete using machine learning algorithms and SHAP, Hybrid Advances 10 (2025). https://doi.org/10.1016/j.hybadv.2025.100483.

[83] R.I. Hamilton, P.N. Papadopoulos, Using SHAP Values and Machine Learning to Understand Trends in the Transient Stability Limit, IEEE Transactions on Power Systems 39 (2024) 1384–1397. https://doi.org/10.1109/TPWRS.2023.3248941.

[84] A.V. Ponce-Bobadilla, V. Schmitt, C.S. Maier, S. Mensing, S. Stodtmann, Practical guide to SHAP analysis: Explaining supervised machine learning model predictions in drug development, Clin Transl Sci 17 (2024). https://doi.org/10.1111/cts.70056.

[85] V.Q. Tran, Predicting and Investigating the Permeability Coefficient of Soil with Aided Single Machine Learning Algorithm, Complexity 2022 (2022). https://doi.org/10.1155/2022/8089428.

[86] X. Xin, G. Hooker, F. Huang, Pitfalls in machine learning interpretability: Manipulating partial dependence plots to hide discrimination, Insur Math Econ 125 (2025). https://doi.org/10.1016/j.insmatheco.2025.103135.

[87] B. Liang, H. Liu, E.L. Cressey, C. Xu, L. Shi, L. Wang, J. Dai, Z. Wang, J. Wang, Uncertainty of Partial Dependence Relationship between Climate and Vegetation Growth Calculated by Machine Learning Models, Remote Sens (Basel) 15 (2023). https://doi.org/10.3390/rs15112920.

[88] P.M. Johnson, W. Barbour, J. V. Camp, H. Baroud, Using machine learning to examine freight network spatial vulnerabilities to disasters: A new take on partial dependence plots, Transp Res Interdiscip Perspect 14 (2022). https://doi.org/10.1016/j.trip.2022.100617.

[89] G. Luo, A review of automatic selection methods for machine learning algorithms and hyperparameter values, Network Modeling Analysis in Health Informatics and Bioinformatics 5 (2016). https://doi.org/10.1007/s13721-016-0125-6.

[90] J.N. Kutz, Machine learning for parameter estimation, Proc Natl Acad Sci U S A 120 (2023). https://doi.org/10.1073/pnas.2300990120.

[91] S.-Z. Li, J.-J. Wang, L. Jiang, R. Deng, Y.-H. Wang, Machine learning-based strength prediction for circular concrete-filled double-skin steel tubular columns under axial compression, Eng Struct 325 (2025) 119460. https://doi.org/10.1016/j.engstruct.2024.119460.

[92] S. Wahab, N.S. Mahmoudabadi, S. Waqas, N. Herl, M. Iqbal, K. Alam, A. Ahmad, Comparative Analysis of Shear Strength Prediction Models for Reinforced Concrete Slab-Column Connections, Advances in Civil Engineering 2024 (2024). https://doi.org/10.1155/2024/1784088.

[93] M. Reza, A. Kakavand, H. Sezen, F. Asce, E. Taciroglu, M. Asce, Data-Driven Models for Predicting the Shear Strength of Rectangular and Circular Reinforced Concrete Columns, (2020). https://doi.org/10.1061/(ASCE).

[94] K. Miao, Z. Pan, A. Chen, Y. Wei, Y. Zhang, Machine learning-based model for the ultimate strength of circular concrete-filled fiber-reinforced polymer–steel composite tube columns, Constr Build Mater 394 (2023). https://doi.org/10.1016/j.conbuildmat.2023.132134.

[95] J. Rahman, K.S. Ahmed, N.I. Khan, K. Islam, S. Mangalathu, Data-driven shear strength prediction of steel fiber reinforced concrete beams using machine learning approach, Eng Struct 233 (2021). https://doi.org/10.1016/j.engstruct.2020.111743.

[96] A. Alghossoon, A. Tarawneh, G. Almasabha, Y. Murad, E. Saleh, H.A. yahia, A.A. yahya, H. Sahawneh, Shear strength of circular concrete-filled tube (CCFT) members using human-guided artificial intelligence approach, Eng Struct 282 (2023). https://doi.org/10.1016/j.engstruct.2023.115820.

[97] Y. Zuhair Murad, Predictive model for bidirectional shear strength of reinforced concrete columns subjected to biaxial cyclic loading, Eng Struct 244 (2021). https://doi.org/10.1016/j.engstruct.2021.112781.

[98] Y. Yu, W. Wu, J. Yan, J. Zang, Probabilistic models for shear strength of circular and square concrete-filled steel tubes, AIP Adv 15 (2025). https://doi.org/10.1063/5.0250829.

[99] C. Cakiroglu, G. Bekdaş, Predictive Modeling of Recycled Aggregate Concrete Beam Shear Strength Using Explainable Ensemble Learning Methods, Sustainability (Switzerland) 15 (2023). https://doi.org/10.3390/su15064957.

[100] T.G. Wakjira, U. Ebead, M.S. Alam, Machine learning-based shear capacity prediction and reliability analysis of shear-critical RC beams strengthened with inorganic composites, Case Studies in Construction Materials 16 (2022). https://doi.org/10.1016/j.cscm.2022.e01008.

[101] A.I. Ioannou, D. Galbraith, N. Bakas, G. Markou, J. Bellos, New Predictive Models for the Computation of Reinforced Concrete Columns Shear Strength, Computers 14 (2025). https://doi.org/10.3390/computers14010002.

Supplementary Files

This is a list of supplementary files associated with this preprint. Click to download.

- CFSTData.xlsx